

Introduction to Nuclear Magnetic Resonance Spectroscopy

Dr Alexey Potapov

University of Nottingham, School of Physics and Astronomy

August 11, 2017

Introduction. Magnetic moment in magnetic field.

- Introduction to Magnetic Resonance
- Applications of NMR
- Magnetic moments in magnetic field.
- Orbital angular momentum operator
- Spin angular momentum operator
- Spin in a magnetic field
- Equilibrium magnetization
- Resonant energy absorption.
- Populations dynamics in two-level system.

1.1. Introduction to Magnetic Resonance

- Magnetic resonance (MR) is a phenomenon of resonant energy absorption by a system of nuclei (and electrons).
- Nuclear magnetic resonance (NMR) results from the intrinsic magnetic moment of the nuclei of some atoms. Magnetic moments of electrons are exploited in electron spin resonance (ESR).
- Magnetic resonance (MR) generally involves placing a sample in a strong magnetic field (to generate polarisation at a fixed resonant frequency) and detecting signals produced following application of pulsed radio-frequency electromagnetic fields (RF pulses).
- MR is a very powerful method for studying the structure of materials: used in physics, chemistry, biology, medicine etc.

1.2. Applications of NMR

- NMR spectroscopy is used for chemical analysis and for molecular structure determination

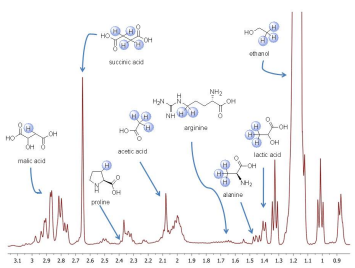


Fig.1: ^1H NMR spectrum of a sample of Spanish wine (<http://www.unirioja.es/gsoe/NMR.htm>)

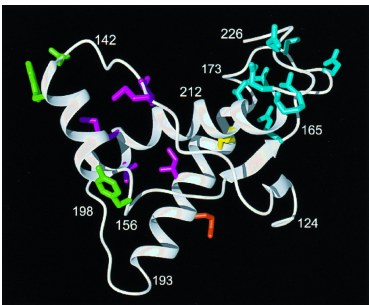


Fig.2: NMR-derived structure of a prion protein <http://www.pnas.org/content/94/14/7281.full>

1.2. Applications of NMR

- NMR relaxometry can be used to monitor molecular environment

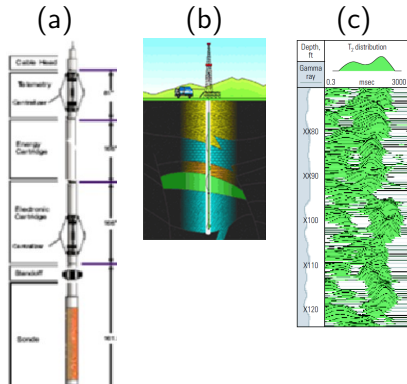


Fig.3: (a) NMR-logging probe, (b) Schematic positioning of the probe in a well, (c) T₂-relaxation profile along the bore. Sources: 1) Allenet al. Oilfield review, Autumn 2000; 2) Coates, Xiao NMR Logging Principles and Applications, Halliburton

1.2. Applications of NMR

- NMR forms the basis for magnetic resonance imaging (MRI)

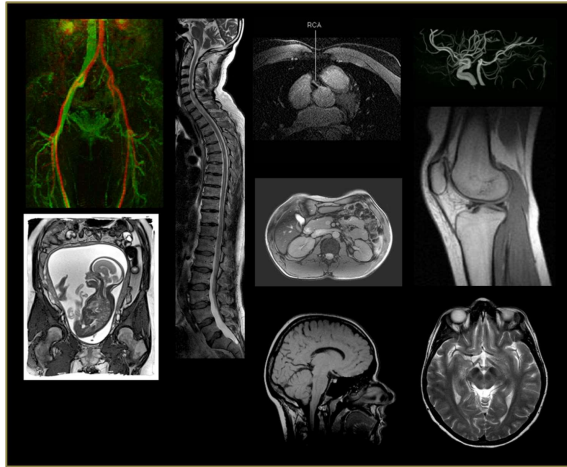


Fig.4: Example magnetic resonance images of blood vessel (in legs), fetus in utero, spine, heart, abdomen, head, blood vessels (in brain), knee, brain (courtesy of Prof. Richard Bowtell)

1.3. Magnetic moments in magnetic field.

How magnetic moments interact with magnetic field? What equations determine the motion?

Consider charges moving in a limited volume. The position of a charge e_n will be given by a vector \mathbf{r}_n and its velocity by \mathbf{v}_n . The overall magnetic moment of such a system is defined as:

$$\mathbf{M} = \frac{1}{2} \sum_n e_n \mathbf{r}_n \times \mathbf{v}_n \quad (1)$$

If all the charges and masses are the same, then \mathbf{M} can be rewritten as:

$$\mathbf{M} = \frac{e}{2m} \sum_n m \mathbf{r}_n \times \mathbf{v}_n = \gamma \mathbf{L}, \quad (2)$$

where

$$\mathbf{L} = \sum_n \mathbf{p}_n \times \mathbf{r}_n \quad (3)$$

is the mechanical angular momentum. **Gyromagnetic ratio** (or magnetogyric):

$$\gamma = \frac{e}{2m} \quad (4)$$

1.3. Magnetic moments in magnetic field.

When a magnetic moment \mathbf{M} is placed into an external uniform permanent magnetic field \mathbf{B} , its energy is given by:

$$E = -\mathbf{M} \cdot \mathbf{B} \quad (5)$$

The torque acting on the system:

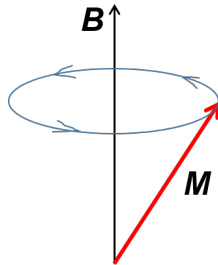
$$\frac{d\mathbf{L}}{dt} = \mathbf{M} \times \mathbf{B} \quad (6)$$

Now using equation 2 we can obtain the equation describing the motion of vector \mathbf{M} :

$$\frac{d\mathbf{M}}{dt} = \gamma \mathbf{M} \times \mathbf{B} \quad (7)$$

1.3. Magnetic moments in magnetic field.

In a uniform magnetic field directed along z -axis $\mathbf{B} = (0, 0, B_0)$, the equation for individual components of \mathbf{M} follow the equations:



$$\begin{aligned}\frac{dM_x}{dt} &= \omega_L M_y \\ \frac{dM_y}{dt} &= -\omega_L M_x \\ \frac{dM_z}{dt} &= 0,\end{aligned}\quad (8)$$

where $\omega_L = \gamma B_0$ - Larmor frequency.

A solution to this system of differential equations with initial values of $M_x(0)$, $M_y(0)$, $M_z(0)$ has the following form:

$$\begin{aligned}M_x(t) &= M_x(0) \cos(\omega_L t) + M_y(0) \sin(\omega_L t) \\ M_y(t) &= -M_y(0) \sin(\omega_L t) + M_y(0) \cos(\omega_L t) \\ M_z(t) &= M_z(0)\end{aligned}\quad (9)$$

1.4. Orbital angular momentum operator

In quantum mechanics physical quantity A is represented by an operator \hat{A} . The mechanical angular momentum is replaced by its corresponding operator:

$$\mathbf{L} = \sum_n \mathbf{p}_n \times \mathbf{r}_n \longleftrightarrow \hat{\mathbf{L}} = \frac{1}{\hbar} \sum_n \hat{\mathbf{r}}_n \times \hat{\mathbf{p}}_n = -i \sum_n \hat{\mathbf{r}}_n \times \nabla_n \quad (10)$$

Angular momentum operator properties. Commutation:

$$[\hat{L}_y, \hat{L}_z] = i\hat{L}_x, [\hat{L}_z, \hat{L}_x] = i\hat{L}_y, [\hat{L}_x, \hat{L}_y] = i\hat{L}_z \quad (11)$$

Angular momentum squared, and its commutation properties:

$$\hat{L}^2 = \hat{L}_x^2 + \hat{L}_y^2 + \hat{L}_z^2 \quad (12)$$

$$[\hat{L}^2, \hat{L}_x] = [\hat{L}^2, \hat{L}_y] = [\hat{L}^2, \hat{L}_z] = 0 \quad (13)$$

1.4. Orbital angular momentum operator

Eigenfunctions of both \hat{L}^2 and \hat{L}_z operators can be characterized by integer quantum numbers l and m respectively. These eigenfunctions will be denoted as $|lm\rangle$. Their eigenvalues are:

$$\hat{L}_z|lm\rangle = m|lm\rangle \quad (14)$$

$$\hat{L}^2|lm\rangle = l(l+1)|lm\rangle \quad (15)$$

Another useful operator are raising and lowering operators:

$$\hat{L}_+ = \hat{L}_x + i\hat{L}_y, \hat{L}_- = \hat{L}_x - i\hat{L}_y \quad (16)$$

$$\langle lm|\hat{L}_+|l(m-1)\rangle = \langle l(m-1)|\hat{L}_-|lm\rangle = \sqrt{(l+m)(l-m+1)} \quad (17)$$

Problem

Calculate $[\hat{L}_+, \hat{L}_x] = ?$, $[\hat{L}_+, \hat{L}_-] = ?$

$$[\hat{L}_y, \hat{L}_z] = i\hat{L}_x, [\hat{L}_z, \hat{L}_x] = i\hat{L}_y, [\hat{L}_x, \hat{L}_y] = i\hat{L}_z$$

$$\hat{L}^2 = \hat{L}_x^2 + \hat{L}_y^2 + \hat{L}_z^2$$

$$[\hat{L}^2, \hat{L}_x] = [\hat{L}^2, \hat{L}_y] = [\hat{L}^2, \hat{L}_z] = 0$$

$$\hat{L}_+ = \hat{L}_x + i\hat{L}_y, \hat{L}_- = \hat{L}_x - i\hat{L}_y$$

Solution

1.4. Orbital angular momentum operator

Classical magnetic moment will have its own quantum analogue, the operator of angular momentum:

$$\mathbf{M} = \gamma \mathbf{L} \longleftrightarrow \hat{\mu} = \gamma \hbar \hat{\mathbf{L}} \quad (18)$$

Given the electron charge $e = 1.6 \cdot 10^{-19} \text{C}$, and mass $m = 9.1 \cdot 10^{-31} \text{kg}$ **Bohr magneton**:

$$\beta_e = \gamma \hbar = \frac{e\hbar}{2m} \approx 9.27 \cdot 10^{-24} \text{J}\cdot\text{T}^{-1} \quad (19)$$

Similarly a **nuclear magneton** could be calculated for a proton (¹H nucleus):

$$\beta = \gamma_N \hbar = \frac{e\hbar}{2m_p} \approx 5.05 \cdot 10^{-27} \text{J}\cdot\text{T}^{-1} \quad (20)$$

1.5. Spin angular momentum operator

However, real nuclei and electrons have spins (intrinsic magnetic moment). Their z-axis projection m takes integer and half-integer values: $m = \frac{1}{2}, 1, \frac{3}{2}, 2$ etc. Similar to the equation for the orbital angular momentum Eq.18. For nuclei spins we get its magnetic moment as:

$$\hat{\mu}_N = \gamma_N \hbar \hat{\mathbf{I}}, \quad (21)$$

where $\hat{\mathbf{I}}$ stands for the nuclear spin operator. All the properties of angular momentum operators listed in Eqs.11-17 will be true for $\hat{\mathbf{I}}$.

1.5. Spin angular momentum operator

Many nuclei in the periodic table are magnetic, i.e. have spin $I \neq 0$. Their magnetic moments could be measured in units of β_N :

$$\hat{\mu}_N = \gamma_N \hbar \hat{\mathbf{I}} = g_N \beta_N \hat{\mathbf{I}}, \quad (22)$$

where g_N - dimensionless g-factor.

Nucleus	Natural abundance %	Nuclear spin (I)	g_N , g-factor	γ_N , Gyromagnetic ratio (10^7 rad/T*s)
1H	99.98	$\frac{1}{2}$	5.585	26.7519
2H	$1.5 \cdot 10^{-2}$	1	0.857	4.1066
^{13}C	1.108	$\frac{1}{2}$	1.405	6.7283
^{14}N	99.635	1	0.403	1.9338
^{15}N	0.365	$\frac{1}{2}$	-0.567	-2.712

Electron magnetic moments can be measured in units of Bohr magnetons: $\hat{\mu}_S = -\gamma_e \hbar \hat{\mathbf{S}} = -g_e \beta_e \hat{\mathbf{S}}$, and for a free electron spin $g_e \approx 2.0023$.

Summary of Lecture 1

- Applications of NMR: chemistry, biology, medicine, industry ...
- Magnetic moment in magnetic field: Classical description
- Recap of angular momentum operator properties:
commutation properties.
- Nuclei have their own nuclear magnetic moment. Described using spin angular momentum operator.

Suggested reading: Harris: 1.1, 1.2, 1.3, 1.4, 1.6, 2.4

1.6. Spin in a magnetic field

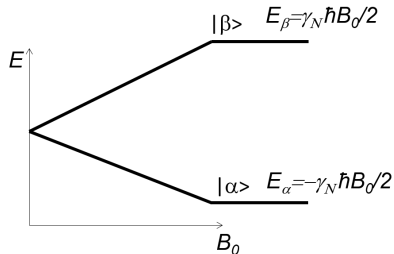
Let's quantum mechanically describe the system of spins in the magnetic field. Eq. 5 can be rewritten in a form of Hamiltonian:

$$E = -\mathbf{M} \cdot \mathbf{B} \longleftrightarrow \mathcal{H} = -\hat{\mu}_N \cdot \mathbf{B} \quad (23)$$

when the magnetic field is directed along z-axis $\mathbf{B} = (0, 0, B_0)$:

$$\mathcal{H} = -\hat{\mu}_N \cdot \mathbf{B} = -\gamma_N \hbar B_0 \hat{I}_z \quad (24)$$

For spin $I = \frac{1}{2}$ such Hamiltonian produces a two-level system. Its energy levels corresponding to eigenfunctions $|\alpha\rangle$ and $|\beta\rangle$:



1.6. Spin in a magnetic field

The transition between the two states requires an energy quantum¹:

$$h\nu_L = \gamma\hbar B_0, \omega_L = \gamma B_0, \nu_L = \frac{\gamma B_0}{2\pi} \quad (25)$$

ω_L and ν_L is the Larmor frequency (angular and cyclic respectively). For simplicity the Hamiltonian \mathcal{H} can be written in frequency units: $\hat{H} = \frac{1}{2\pi\hbar}\mathcal{H} = \nu_L \hat{I}_z$.

Nucleus	Natural abundance %	Nuclear spin (I)	Larmor frequency at 11.744T, MHz	γ_N , Gyromagnetic ratio (10^7 rad/T*s)
^1H	99.98	$\frac{1}{2}$	500	26.7519
^2H	1.5×10^{-2}	1	76.753	4.1066
^{13}C	1.108	$\frac{1}{2}$	125.721	6.7283
^{14}N	99.635	1	36.118	1.9338
^{15}N	0.365	$\frac{1}{2}$	50.664	-2.712

1.7. Equilibrium magnetization

NMR measurements are generally made on bulk samples which contain very large numbers of nuclear spins (e.g. 1 cm³ contains $N \approx 6.7 \cdot 10^{22}$ ¹H atoms) The measured signals therefore result from the collective effect of a large number of magnetic moments that can be described using a bulk magnetization. At thermal equilibrium, the numbers of nuclei in the | α \rangle state N_α and | β \rangle state N_β follow Boltzmann distribution:

$$\frac{N_\alpha}{N_\beta} = e^{-\frac{\gamma B_0}{kT}} \approx (1 - \frac{\gamma B_0}{kT}), \quad (26)$$

when $\gamma B_0 \ll kT$. Overall magnetization then can be calculated as:

$$M_z = N_\alpha(-\frac{1}{2}\gamma\hbar) + N_\beta(\frac{1}{2}\gamma\hbar) = N\frac{\gamma^2\hbar^2B_0}{4kT} \quad (27)$$

Problem

- What is the value of $\frac{\gamma_N \hbar B_0}{kT}$ for proton nuclei (${}^1\text{H}$) at 9.4 T magnetic field at 300 K?
- What is the value of $\frac{\gamma_e \hbar B_0}{kT}$ electron (${}^1\text{H}$) at 9.4 T magnetic field at 4 K?

Electron charge

$$e = 1.602 \cdot 10^{-19} \text{ C}$$

Electron mass

$$m_e = 9.109 \cdot 10^{-31} \text{ kg}$$

Proton mass

$$m_p = 1.673 \cdot 10^{-27} \text{ kg}$$

Plank constant

$$\hbar = 1.054 \cdot 10^{-34} \frac{\text{J} \cdot \text{s}}{\text{rad}}$$

Proton g-factor

$$g_p = 5.585$$

Electron g-factor

$$g_e = 2.0023$$

Nuclear magneton

$$\beta_N = 5.05 \cdot 10^{-27} \text{ J} \cdot \text{T}^{-1}$$

Bohr magneton

$$\beta_e = 9.27 \cdot 10^{-24} \text{ J} \cdot \text{T}^{-1}$$

Proton gyromagnetic ratio

$$\gamma_N = 26.7519 \cdot 10^7 \frac{\text{rad}}{\text{T} \cdot \text{s}}$$

Electron gyromagnetic ratio

$$\gamma_e = 1.76 \cdot 10^{11} \frac{\text{rad}}{\text{T} \cdot \text{s}}$$

Boltzmann constant

$$k = 1.38 \cdot 10^{-23} \text{ J} \cdot \text{K}^{-1}$$

Avogadro's constant

$$N_A = 6.023 \cdot 10^{23} \text{ mol}^{-1}$$

1.8. Resonant energy absorption.

How does a system of spins interact with electromagnetic interaction?

Let's apply oscillating magnetic field to our system. A spin system Hamiltonian becomes time-dependent and for an oscillation along the x -axis we obtain:

$$\begin{aligned}\mathcal{H}(t) &= -\hat{\mu}(\mathbf{B}_0 + \mathbf{B}(t)) = \\ &= -\gamma\hbar\hat{I}_z(B_0 + B_1(t)) = \\ &= -\gamma\hbar\hat{I}_zB_0 - \gamma\hbar\hat{I}_x B_1 \cos(\omega t),\end{aligned}\tag{28}$$

where H_1 and ω are the amplitude and the frequency of the oscillating magnetic field. According to perturbation theory the transition probability between the initial state $|a\rangle$ and the final state $|b\rangle$ with a time dependent Hamiltonian $\hat{V}(t) = 2\hat{F} \cos(\omega t)$ is (Fermi's golden rule):

$$P_{ab} = \frac{2\pi}{\hbar} |\langle a | \hat{F} | b \rangle|^2 \delta(E_{ab} - \hbar\omega),\tag{29}$$

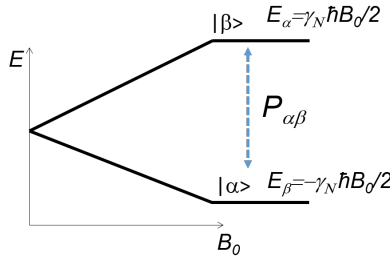
where $E_{ab} = E_a - E_b$ is an energy difference between the energies of levels a and b .

Note! The matrix element $|\langle a | \hat{F} | b \rangle|$ represents the selection rules for various levels, if it equals to zero, the transition is forbidden, otherwise - allowed.

1.9. Populations dynamics in two-level system.

For a two level system described before, the matrix element $\langle \alpha | \hat{I}_x | \beta \rangle = \frac{1}{2}$. The transition probability then becomes:

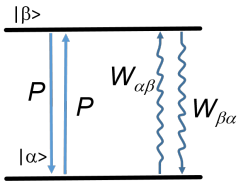
$$P_{\alpha\beta} = \frac{\pi}{2\hbar} (\gamma H_1)^2 \delta(E_{\alpha\beta} - \hbar\omega), \quad (30)$$



The effect of resonant absorption (and emission) of electromagnetic irradiation at the frequency matching the energy difference in a nuclear system is called Nuclear Magnetic Resonance (NMR).

1.9. Populations dynamics in two-level system.

In a two-level system the transition will take place due to the action of external irradiation, but also due to interaction with the environment.



P - the rate of transitions driven by external field, $W_{\alpha\beta}, W_{\beta\alpha}$ - rates of spontaneous spin flips due to interaction with environment. In thermal equilibrium:

$$N_\alpha^0 W_{\alpha\beta} = N_\beta^0 W_{\beta\alpha}, \text{i.e.} \quad (31)$$

$$\frac{W_{\beta\alpha}}{W_{\alpha\beta}} = \exp^{-\frac{\gamma\hbar B_0}{kT}} \approx 1 - \frac{\gamma\beta B_0}{kT} \quad (32)$$

1.9. Populations dynamics in two-level system.

Equation for populations of levels:

$$\begin{aligned}\frac{dN_\alpha}{dt} &= -N_\alpha(P + W_{\alpha\beta}) + N_\beta(P + W_{\beta\alpha}) \\ \frac{dN_\beta}{dt} &= N_\alpha(P + W_{\alpha\beta}) - N_\beta(P + W_{\beta\alpha})\end{aligned}\tag{33}$$

If we introduce the average rate of spontaneous transitions

$$W = \frac{1}{2}(W_{\alpha\beta} - W_{\beta\alpha}), \text{ then } W_{\alpha\beta} = W\left(1 + \frac{\gamma\hbar B_0}{2kT}\right) \text{ and}$$

$$W_{\beta\alpha} = W\left(1 - \frac{\gamma\hbar B_0}{2kT}\right), \text{ the equations can be rewritten:}$$

$$\begin{aligned}\frac{dN_\alpha}{dt} &= (N_\beta - N_\alpha)P + (N_\beta - N_\alpha)W - W\frac{\gamma\beta B_0}{2kT}N \\ \frac{dN_\beta}{dt} &= -(N_\beta - N_\alpha)P - (N_\beta - N_\alpha)W + W\frac{\gamma\beta B_0}{2kT}N\end{aligned}\tag{34}$$

1.9. Populations dynamics in two-level system.

Denote the population difference as $n = N_\beta - N_\alpha$ and thermal equilibrium population difference $n_0 = N_\beta^0 - N_\alpha^0 \approx N \frac{\gamma \hbar B_0}{2kT}$ the equations can be rewritten as:

$$\frac{dn}{dt} = -2nP - 2nW + 2Wn_0, \quad (35)$$

or

$$\frac{dn}{dt} = -2nP - \frac{(n - n_0)}{T_1}, \quad (36)$$

where $T_1 = \frac{1}{2W}$ is called **spin-lattice relaxation time** determines how quickly a spin system reaches a thermal equilibrium with environment. In equilibrium, when $\frac{dn}{dt} = 0$:

$$n = \frac{n_0}{1 + 2PT_1} \quad (37)$$

when the power is very large $PT_1 \gg 1$, $n \rightarrow 0$, i.e. the system is **saturated** and no signal can be observed.

Summary of Lecture 2

- Spin $I = \frac{1}{2}$ in a magnetic field. Two-level system.
- System of spins in a magnetic field is capable of absorbing radiation at a resonant frequency.
- Population dynamics in a two-level system. Signal as function of radiation power and saturation.

Suggested reading: Harris 1.5, 1.7, Slichter 1.3

Harris 1.20 - CW NMR spectrometer

Chemical shifts and J-couplings. NMR spectra in liquids.

- Chemical shifts.
- J-couplings.
- J-couplings in AX system.
- Interpreting simple NMR spectra
- Range of J-couplings. Are they useful for structure determination?
- Heteronuclear J-couplings.
- J-coupling in equivalent system.
- J-coupling in AB system.

2.1. Chemical shifts.

Electrons in atoms in molecules interact with external magnetic field and in turn produce their own magnetic field B_0 . The Larmor frequency get shifted in a chemical specific manner - this is known as the **chemical shift**. The spin Hamiltonian for a nucleus is:

$$\hat{H} = -\gamma_N \hbar (1 - \sigma) B_0 \hat{I}_z, \quad (38)$$

Classical illustration of diamagnetic chemical shift:

$$\omega = \frac{e}{2m_e} B_0$$

$$j = -e[\omega \times r]\rho_e = -\frac{e^2}{2m_e} [B_0 \times r]\rho_e$$

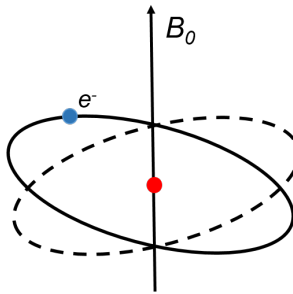
$$dB_i = \frac{\mu_0}{4\pi r^3} [j \times r] dV$$

$$dB_i = -\frac{\mu_0 e^2}{8\pi m_e r^3} [[B_0 \times r] \times r] \rho_e dV$$

$$B_{iz} = -B_0 \frac{\mu_0 e^2}{8\pi m_e} \int \rho_e \frac{x^2 + y^2}{r^3} dV$$

Quantum mechanical result:

$$\sigma = -\frac{\mu_0 e^2}{8\pi m_e} \langle \Psi | \frac{x^2 + y^2}{r^3} | \Psi \rangle$$



2.1. Chemical shifts.

Let's calculate the effect of ring current in cyclic aromatic molecules. Consider benzene molecule:

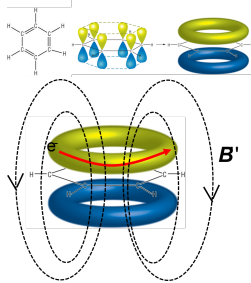


Fig.5: (top) Schematic representation of electron orbitals in a benzene molecule, (bottom) local fields in a benzene molecule produced by electron currents induced by a magnetic field.

Larmor precession frequency of electrons $\omega_L = \frac{eB_0}{2m_e}$. Current can be calculated as charge $6e$, divided by precession period $\frac{2\pi}{\omega_L}$:

$$i = \frac{3e^2 B_0}{2\pi m_e} \quad (39)$$

Circular conductor creates a magnetic moment $\mu = i \cdot \pi r^2$, totalling in:

$$\mu = -\frac{3e^2 B_0 r^2}{2m_e} \quad (40)$$

The magnetic field created by a magnetic moment $\mathbf{B} = \frac{\mu_0}{4\pi} \left(\frac{\mathbf{r}(mr)}{r^5} - \frac{\mathbf{m}}{r^3} \right)$ reduces to:

$$B_i = -\frac{\mu_0}{4\pi} \frac{m}{r^3} = \frac{3\mu_0 e^2}{8\pi} \frac{r^2}{(r+d)^3} B_0 \quad (41)$$

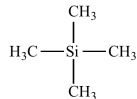
$$\sigma = -\frac{\mu_0}{4\pi m_e} \frac{m}{r^3} = \frac{3\mu_0 e^2}{8\pi} \frac{r^2}{(r+d)^3} \quad (42)$$

Given benzene molecule radius $r = 1.4 \text{ \AA}$, CH-bond length $d = 1.1 \text{ \AA}$ we obtain:

$$\sigma \approx -5.3 \cdot 10^{-6}, \sigma_{iso} \approx -1.8 \cdot 10^{-6} \quad (43)$$

2.1. Chemical shifts.

Chemical shifts are usually measured in ppm's and are referenced with respect to the signals of tetramethylsilane (TMS).



$$\delta = \frac{\nu_{\text{sample}} - \nu_{\text{TMS}}}{\nu_{\text{TMS}}} \times 10^6 \text{ ppm} \quad (44)$$

$$\delta = (\sigma_{\text{TMS}} - \sigma_{\text{sample}}) \times 10^6 \text{ ppm} \quad (45)$$

In general the ${}^1\text{H}$ chemical shift is greater for nuclei to atoms/bonds that reduce the electron density at the atom.

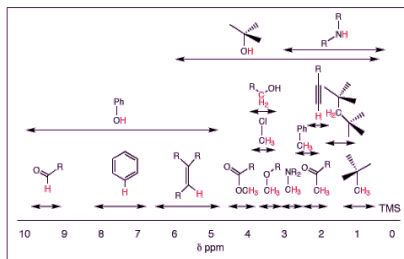


Fig.6: Chemical shifts in various organic molecules Source: <http://orgchem.colorado.edu/Spectroscopy/nmrtheory/protonchemshift.html>

2.1. Chemical shifts.

Consider the ^1H -spectrum of methyl acetate.

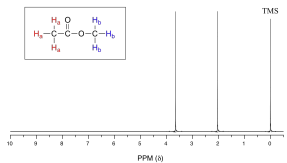


Fig.7: ^1H spectrum of methyl acetate. Source: http://chemwiki.ucdavies.edu/Organic_Chemistry

- the TMS appears at 0 ppm
- chemical shift increases from right to left
- two resonances correspond to protons of the two methyl groups
- the presence of electronegative oxygen atom in methoxy group produces weaker shielding (σ) thus makes bigger chemical shift δ
- three nuclei of methyl groups resonate at the same frequency. Peak heights are the same.

2.1. Chemical shifts.

For other nuclei, paramagnetic shifts which arise from mixing of excited state with the ground state due to the effect of the applied field, B_0 on the Hamiltonian can be important, and the range of chemical shifts is usually larger than for ^1H nuclei.

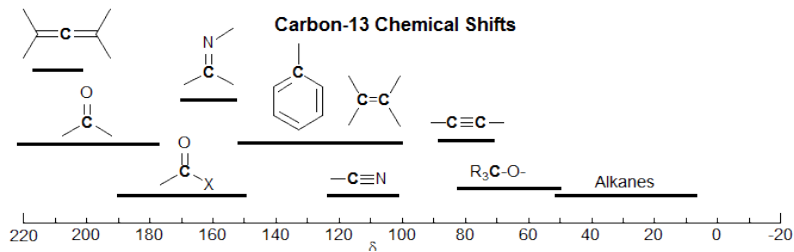


Fig.8: ^{13}C chemical shifts, <https://www.chem.wisc.edu/areas/reich/nmr/>

2.2. J-couplings.

Nuclear spins interact with one another. In solution, one prominent spin-spin interaction is called **J-coupling**.

This intra-molecular scalar coupling is caused by the combination of two effects: the Pauli principle means that the electrons in the bond have opposite spin-state (spin-up and spin-down), while hyperfine couplings (specifically Fermi contact interaction) means that it is energetically favourable for each nuclear spin to be anti-parallel to the electron spin.

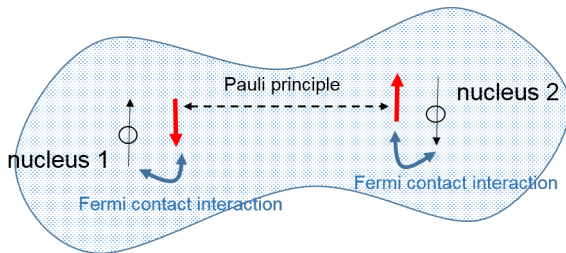


Fig.9: Origin of J-couplings. Low energy configuration in which nuclear spins are antiparallel

2.2. J-couplings.

Let's find the eigenstates of a Hamiltonian with J-coupling

Hamiltonian of J-coupling in solution (all anisotropy is averaged):

$$\begin{aligned}\hat{H} &= J\hat{\mathbf{I}}_1 \cdot \hat{\mathbf{I}}_2 = J(\hat{I}_{1x}\hat{I}_{2x} + \hat{I}_{1y}\hat{I}_{2y} + \hat{I}_{1z}\hat{I}_{2z}) = \\ &= J\hat{I}_{1z}\hat{I}_{2z} + \frac{J}{2}(\hat{I}_{1+}\hat{I}_{2-} + \hat{I}_{1-}\hat{I}_{2+})\end{aligned}\quad (46)$$

J is usually measured in units of frequency, i.e. Hz.

In frequency units the full spin Hamiltonian for a system of two nuclei A and B of the same kind would be:

$$\hat{H} = -\nu_0(1-\sigma_A)\hat{I}_{Az} - \nu_0(1-\sigma_B)\hat{I}_{Bz} + J\hat{I}_{Az}\hat{I}_{Bz} + \frac{J}{2}(\hat{I}_{A+}\hat{I}_{B-} + \hat{I}_{A-}\hat{I}_{B+})\quad (47)$$

2.2. J-couplings.

Let's find the eigenstates of a Hamiltonian with J-coupling

For two coupled spins $\frac{1}{2}$ the Hamiltonian matrix in the basis of functions $|1\rangle = |\alpha_1\alpha_2\rangle, |2\rangle = |\alpha_1\beta_2\rangle, |3\rangle = |\beta_1\alpha_2\rangle, |4\rangle = |\beta_1\beta_2\rangle$
The Hamiltonian matrix of such a system are:

$$H_{ik} = \langle i|\hat{H}|k\rangle = \begin{bmatrix} -\frac{\nu_A + \nu_B}{2} + \frac{J}{4} & 0 & 0 & 0 \\ 0 & -\frac{\nu_A - \nu_B}{2} - \frac{J}{4} & \frac{J}{2} & 0 \\ 0 & \frac{J}{2} & \frac{\nu_A - \nu_B}{2} - \frac{J}{4} & 0 \\ 0 & 0 & 0 & -\frac{\nu_A + \nu_B}{2} + \frac{J}{4} \end{bmatrix} \quad (48)$$

when $|\nu_A - \nu_B| \gg J$ the off-diagonal terms due to $\hat{I}_{A\pm}\hat{I}_{B\mp}$ can be neglected. That is called **AX system**. When off-diagonal terms cannot be neglected, we deal with a so called **AB system**. Let's consider nuclei of the same type (i.e. both ^1H or both ^{13}C). When $\gamma_N \hbar |\omega_1 - \omega_2| \ll J$,

2.2. J-couplings.

For two coupled spins $\frac{1}{2}$ the Hamiltonian matrix in the basis of functions $|1\rangle = |\alpha_1\alpha_2\rangle, |2\rangle = |\alpha_1\beta_2\rangle, |3\rangle = |\beta_1\alpha_2\rangle, |4\rangle = |\beta_1\beta_2\rangle$
 The Hamiltonian matrix of such a system are:

$$H_{ik} = \langle i|\hat{H}|k\rangle = \begin{bmatrix} -\frac{\nu_A + \nu_B}{2} + \frac{J}{4} & 0 & 0 & 0 \\ 0 & -\frac{\nu_A - \nu_B}{2} - \frac{J}{4} & \frac{J}{2} & 0 \\ 0 & \frac{J}{2} & \frac{\nu_A - \nu_B}{2} - \frac{J}{4} & 0 \\ 0 & 0 & 0 & -\frac{\nu_A + \nu_B}{2} + \frac{J}{4} \end{bmatrix} \quad (49)$$

when $|\nu_A - \nu_B| \gg J$ the off-diagonal terms due to $\hat{I}_{A\pm}\hat{I}_{B\mp}$ can be neglected. That is called **AX system**. When off-diagonal terms cannot be neglected, we deal with a so called **AB system**.

Let's consider nuclei of the same type (i.e. both ^1H or both ^{13}C). When $\gamma_N \hbar |\omega_1 - \omega_2| \ll J$,

2.3. J-couplings in AX system.

Eq.29 is non-zero when corresponding matrix element is not zero.
The selection rules for two nuclei then : $\langle i | \hat{I}_{1x} + \hat{I}_{2x} | k \rangle \neq 0$.

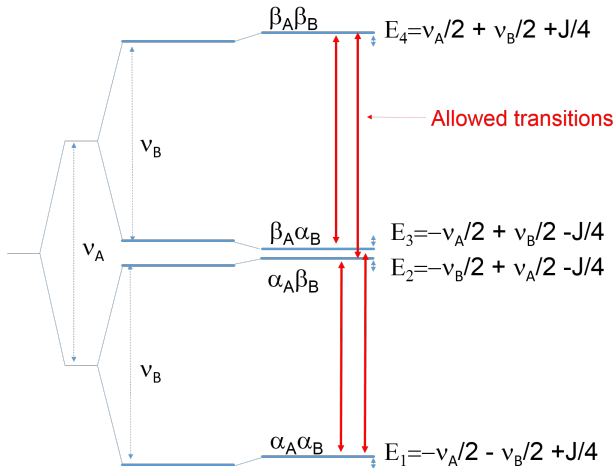


Fig.10: Level diagram for two J-coupled spins in AX system

2.3. J-couplings in AX system.

In a more general case, when $I_A, I_B \neq \frac{1}{2}$, the energy levels follow the following equation:

$$E = -\nu_A m_1 - \nu_0(1 - \sigma_B)m_2 + Jm_1m_2 \quad (50)$$

The allowed transitions for spin A have the following frequencies:

$$\nu = \nu_A + m_B J, \quad (51)$$

where $m_B = -I_B, -(I_B - 1) \dots (I_B - 1)$, I_B is the projection of nuclear spin B. The resonance line is therefore being split into several components. Similarly, for spin B:

$$\nu = \nu_B + m_A J, \quad (52)$$

2.4. Interpreting simple NMR spectra

For one coupled nucleus:

$$\nu = \nu_A + m_B J, \quad (53)$$

For two coupled nuclei:

$$\nu = \nu_A + m_B J + m_C J, \quad (54)$$

For three:

$$\nu = \nu_A + m_B J + m_C J + m_D J, \quad (55)$$

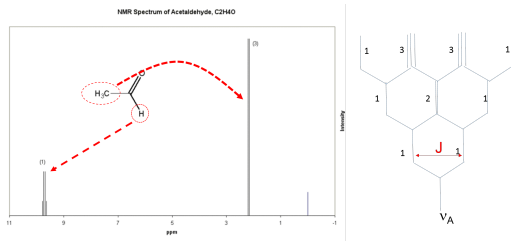
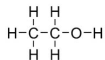


Fig.11: Spectrum of acetaldehyde. Source: <https://chem242.wikispaces.com>

2.4. Interpreting simple NMR spectra

Problem

Draw schematically ^1H spectrum of ethyl alcohol? Proton Larmor frequency is 90 MHz (i.e. treat as AX system).



$\delta_{\text{CH}_3} = 1.22 \text{ ppm}$, $\delta_{\text{CH}_2} = 3.68 \text{ ppm}$, $\delta_{\text{OH}} = 2.61 \text{ ppm}$,
consider only $J_{\text{CH}_2-\text{CH}_3} = 7.29 \text{ Hz}$.

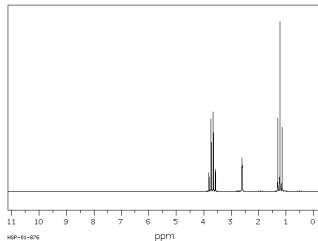


Fig.12: Ethanol spectrum at 90 MHz in CDCl_3

2.5. Range of J-couplings. Are they useful for structure determination?

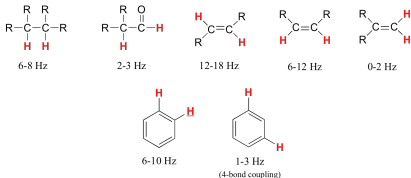


Fig.13: Typical J-couplings https://chem.libretexts.org/Textbook_Maps/Organic_Chemistry_Textbook_Maps/

Is there any simple meaning to J-couplings? **Karplus equation** is an empiric formula for J coupling as a function of a dihedral angle ϕ .

$$J = A \cos \phi + B \cos 2\phi + C \quad (56)$$

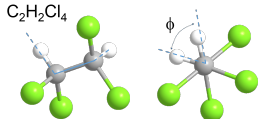


Fig.14: Dihedral angle in 1,1,2,2-tetrachlorethane

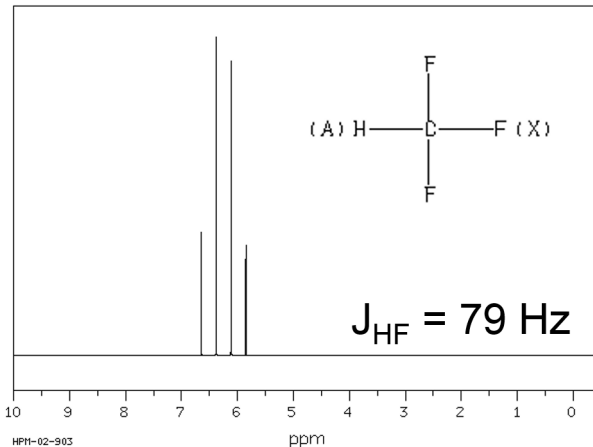
2.6. Heteronuclear J-couplings.

Heteronuclear systems are automatically AX systems, i.e.

$$|\nu_A - \nu_B| \gg J.$$

Example: trifluoromethane (fluoroform)

^1H NMR spectrum



Summary of lecture 3.

- J-couplings and chemical shift to an extent are unique in different molecules, and NMR spectra help in identifying chemical compounds by their spectra.
- Chemical shifts originate from magnetic field shielding by electrons.
- CS report on the chemical environment of a nucleus
- J-couplings cause spectral splittings.

Suggested reading: Harris 1.8, 1.9, 1.11, 1.12, 1.13, 8.2, 8.9., 8.23

For more detailed quantum mechanical theory of chemical shifts: Slichter 4.1-4.5, for detailed theory of J-couplings: Slichter 4.9

2.7. J-coupling in equivalent system.

Are protons in CH₃ or CH₂ groups coupled to one another?

Yes. But they are equivalent and therefore not observed.

$$\hat{H} = -\nu_0(\hat{I}_{1z} + \hat{I}_{2z} + \hat{I}_{3z}) + J(\mathbf{I}_1\mathbf{I}_2 + \mathbf{I}_2\mathbf{I}_3 + \mathbf{I}_1\mathbf{I}_3) \quad (57)$$

Let's rewrite the last term as:

$$\mathbf{I}_1\mathbf{I}_2 + \mathbf{I}_2\mathbf{I}_3 + \mathbf{I}_1\mathbf{I}_3 = \frac{1}{2}(\mathbf{I}_1 + \mathbf{I}_2 + \mathbf{I}_3)^2 - \frac{1}{2}(\mathbf{I}_1^2 + \mathbf{I}_2^2 + \mathbf{I}_3^2) \quad (58)$$

We can introduce new operator: $\mathbf{F} = \mathbf{I}_1 + \mathbf{I}_2 + \mathbf{I}_3$. Given that

$I_1 = I_2 = I_3 = \frac{1}{2}$ the Hamiltonian can be rewritten using this new operator:

$$\hat{H} = -\nu_0 \hat{F}_z + J(\mathbf{F}^2 - \frac{9}{4}) \quad (59)$$

Eigenfunctions of this Hamiltonian are functions $|FM_F\rangle$, where

$$F = \frac{1}{2} \text{ or } \frac{3}{2}.$$

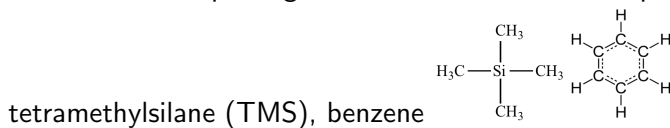
2.7. J-coupling in equivalent system.

$$\hat{H} = -\nu_0 \hat{F}_z + J(\mathbf{F}^2 - \frac{9}{4}) \quad (60)$$

Selection rules for transitions: $\langle i | \hat{F}_x | k \rangle \neq 0$, since $\hat{F}_x = \frac{\hat{F}_+ + \hat{F}_-}{2}$,

the selection rules then are: $\langle i | \hat{F}_{\pm} | k \rangle \neq 0$. Since $\hat{F}_{\pm} = \text{const} | F_M F \pm 1 \rangle$, the allowed transition does not change the second term in Eq.60.

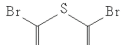
Strictly speaking if a molecule contains only nuclei of one type, and no other J -splitting will not be observed. Examples:



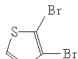
2.7. J-coupling in equivalent system.

Problem

Sketch the ^1H NMR spectra of 2,3-dibromothiophene and 2,5-dibromothiophene? ^{79}Br and ^{81}Br are quadrupolar nuclei, and their J-couplings can be ignored.

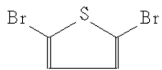


2,5 -dibromothiophene

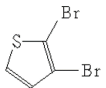


2,3 -dibromothiophene

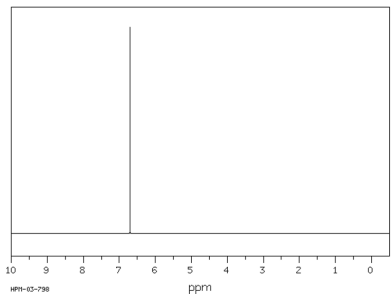
2.7. J-coupling in equivalent system.



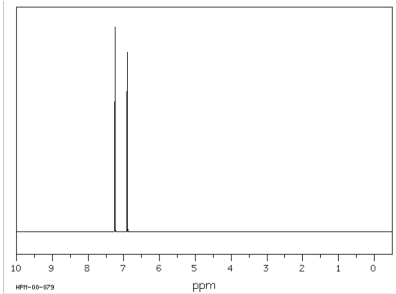
2,5 -dibromothiophene



2,3 -dibromothiophene



HPN-03-798



HPN-00-079

2.8. J-coupling in AB system.

What happens if $\nu_A - \nu_B \gg J$ is no longer true?

The matrix of spin Hamiltonian is:

$$\begin{bmatrix} -\frac{\nu_A + \nu_B}{2} + \frac{J}{4} & 0 & 0 & 0 \\ 0 & -\frac{\nu_A - \nu_B}{2} - \frac{J}{4} & \frac{J}{2} & 0 \\ 0 & \frac{J}{2} & \frac{\nu_A - \nu_B}{2} - \frac{J}{4} & 0 \\ 0 & 0 & 0 & -\frac{\nu_A + \nu_B}{2} + \frac{J}{4} \end{bmatrix} \quad (61)$$

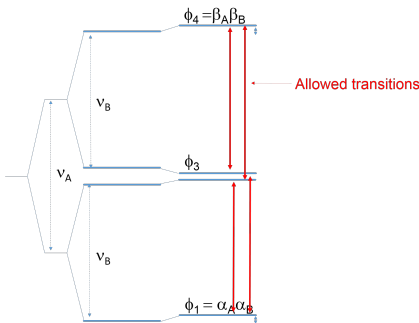
The general way of solving is finding the eigenvalues and eigenvalues and eigenfunctions of this Hamiltonian. the solution can be represented by following replacements:

$$\begin{aligned} \frac{\nu_A - \nu_B}{2} &= \frac{\delta}{2} = C \cos 2\theta \\ \frac{J}{2} &= C \sin 2\theta \\ C &= \frac{1}{2} \sqrt{\delta^2 + J^2}, \tan 2\theta = \frac{J}{\delta}, \bar{\nu} = \frac{\nu_A + \nu_B}{2} \end{aligned} \quad (62)$$

2.8. J-coupling in AB system.

In this notation the eigenvalues and eigenfunctions are:

$$\begin{aligned} E_1 &= -\bar{\nu} + \frac{J}{4} & \phi_1 &= |\alpha_A\alpha_B\rangle \\ E_2 &= -\frac{J}{4} - C & \phi_2 &= \sin\theta|\alpha_A\beta_B\rangle - \cos\theta|\beta_1\alpha_2\rangle \\ E_3 &= -\frac{J}{4} + C & \phi_3 &= \cos\theta|\alpha_A\beta_B\rangle + \sin\theta|\beta_1\alpha_2\rangle \\ E_4 &= \bar{\nu} + \frac{J}{4} & \phi_4 &= |\beta_A\beta_B\rangle \end{aligned} \quad (63)$$



Problem

Calculate the transition probability between levels 1 and 2?
(Hint: use Eq.29)

Fig.15: Level diagram for AB system of J-coupled nuclei.

2.8. J-coupling in AB system.

Problem

Calculate the transition probability between levels 1 and 2? (Hint: use Eq.29)

For transition $1 \leftrightarrow 2$ we have:

$$\begin{aligned} I_{1\leftrightarrow 2} &\sim | \langle 1 | \hat{I}_{Ax} + \hat{I}_{Bx} | 2 \rangle |^2 = \\ &= \langle 1 | \frac{\hat{I}_{A+} + \hat{I}_{A-}}{2} + \frac{\hat{I}_{B+} + \hat{I}_{B-}}{2} | 2 \rangle^2 = \\ &= \left(\langle \alpha_A \alpha_B | \frac{\hat{I}_{A+} + \hat{I}_{A-}}{2} + \frac{\hat{I}_{B+} + \hat{I}_{B-}}{2} | \sin \theta | \alpha_A \beta_B \rangle + \cos \theta | \beta_A \alpha_B \rangle \right)^2 = \\ &= \left(\frac{\cos \theta + \sin \theta}{2} \right)^2 = \frac{1 + \sin 2\theta}{4} \end{aligned} \tag{64}$$

2.8. J-coupling in AB system.

For all the transitions we obtain:

Transition	Frequency	Intensity:
$4 \leftrightarrow 2$	$\bar{\nu} + C + \frac{J}{2}$	$\frac{1 - \sin 2\theta}{1 + \sin 2\theta}$
$3 \leftrightarrow 1$	$\bar{\nu} + C - \frac{J}{2}$	$\frac{1 + \sin 2\theta}{1 - \sin 2\theta}$
$4 \leftrightarrow 3$	$\bar{\nu} - C + \frac{J}{2}$	$\frac{1 + \sin 2\theta}{1 - \sin 2\theta}$
$2 \leftrightarrow 1$	$\bar{\nu} - C - \frac{J}{2}$	$\frac{4}{1 - \sin 2\theta}$

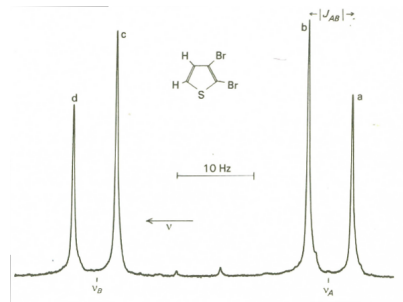


Fig.16: 100 MHz ^1H NMR spectrum of 2,3-dibromothiophene, $| \nu_A - \nu_B | = 30.5 \text{ Hz}$, $J = 5.7 \text{ Hz}$

2.8. J-coupling in AB system.

For all the transitions we obtain:

Transition	Frequency	Intensity:
$4 \leftrightarrow 2$	$\bar{\nu} + C + \frac{J}{2}$	$\frac{1 - \sin 2\theta}{4}$
$3 \leftrightarrow 1$	$\bar{\nu} + C - \frac{J}{2}$	$\frac{1 + \sin 2\theta}{4}$
$4 \leftrightarrow 3$	$\bar{\nu} - C + \frac{J}{2}$	$\frac{1 + \sin 2\theta}{4}$
$2 \leftrightarrow 1$	$\bar{\nu} - C - \frac{J}{2}$	$\frac{1 - \sin 2\theta}{4}$

Consider following scenarios:

1. $J \ll \delta$ means that $\sin 2\theta \ll 1$ and $C \approx \frac{\delta}{2}$. The leads to AX system shown Fig.52B
2. $\delta \ll J$ means that $\sin 2\theta \approx 1$. A strong doublet and two weak satellite lines in Fig.52C.

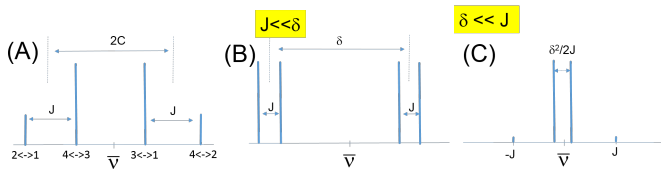


Fig.17: Schematic spectra in several cases (A) $|\nu_A - \nu_B| \sim J$, (B) weakly coupled nuclei $|\nu_A - \nu_B| \gg J$, (C) very weak J-coupling $|\nu_A - \nu_B| \ll J$

2.8. J-coupling in AB system.

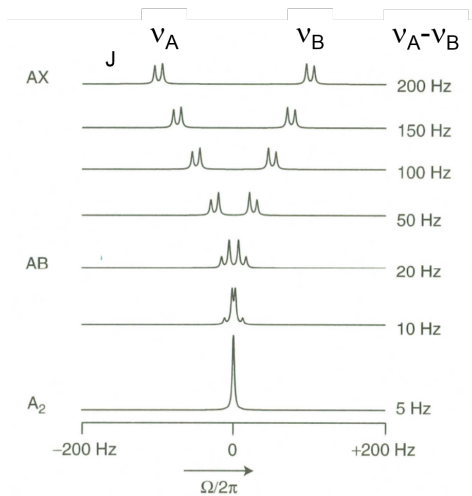


Fig.18: Spectra of spin $\frac{1}{2}$ pairs for $J = 10$ Hz as a function of Larmor frequency difference.

Summary of Lecture 4.

- Splittings in equivalent systems are not observed.
- The case of strong J-couplings can be treated exactly.

Suggested reading: Harris 1.14, 2.17, 2.10

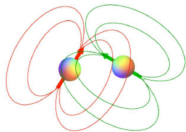
NMR spectra of solids.

- Dipolar coupling Hamiltonian.
- Powder spectra of dipolar coupled nuclei.
- Chemical shift anisotropy.
- Magic angle spinning.
- Quadrupolar interaction.

3.1. Dipolar coupling Hamiltonian.

- Nuclear magnetic moments of nuclei interact via dipolar interaction. (It is averaged to zero in liquids). Classical expression for such interaction is:

$$E = -(\mathbf{m}_1 \mathbf{B}_{dip}) = \\ = \frac{\mu_0}{4\pi} \left(\frac{3(\mathbf{m}_1 \mathbf{r})(\mathbf{m}_2 \mathbf{r})}{r^5} - \frac{\mathbf{m}_1 \mathbf{m}_2}{r^3} \right),$$



- The field induced by another one proton at the location of other proton spaced apart by 1.6 Å is $B_{dip} \sim \frac{m}{r^3} \approx 0.7 \text{ mT}$ or $\frac{g_N \beta_N B_{dip}}{2\pi\hbar} \approx 30 \text{ kHz}$.
- In quantum mechanics the magnetic moments $\mathbf{m}_1, \mathbf{m}_2$ are replaced with operators $g_{1,2}\beta_{1,2}\hat{l}_{1,2} = \gamma_{1,2}\hbar\hat{l}_{1,2}$, giving rise to a

3.1. Dipolar coupling Hamiltonian.

Expanding the spin operator products and using spherical polar coordinates (r, θ, ϕ) :

$$\hat{H}_{dip} = \frac{\mu_0}{8\pi^2} \frac{\gamma_1 \gamma_2 \hbar}{r^3} (A + B + C + D + E + F), \text{ where} \quad (66)$$

$$\begin{aligned} A &= -\hat{l}_{1z}\hat{l}_{2z}(3\cos^2\theta - 1) \\ B &= \frac{1}{4}(\hat{l}_{1+}\hat{l}_{2-} + \hat{l}_{1-}\hat{l}_{2+})(3\cos^2\theta - 1) \\ C &= -\frac{3}{2}(\hat{l}_{1z}\hat{l}_{2+} + \hat{l}_{1+}\hat{l}_{2z})\sin\theta\cos\theta e^{-i\phi} \\ D &= -\frac{3}{2}(\hat{l}_{1z}\hat{l}_{2-} + \hat{l}_{1-}\hat{l}_{2z})\sin\theta\cos\theta e^{i\phi} \\ E &= -\frac{3}{4}\hat{l}_{1+}\hat{l}_{2+}\sin^2\theta e^{-i2\phi} \\ F &= -\frac{3}{4}\hat{l}_{1-}\hat{l}_{2-}\sin^2\theta e^{i2\phi} \end{aligned} \quad (67)$$

Each of these terms is a product of a combination of spin operator products with geometrical factor, that depends on θ and ϕ . Only A commutes with the two-spin Zeeman Hamiltonian.

3.1. Dipolar coupling Hamiltonian.

In liquids the dipolar interaction rapidly fluctuates due to molecular reorientation

Problem

Show that dipolar interaction terms averaged over many orientations are zero.

3.1. Dipolar coupling Hamiltonian.

The spin Hamiltonian of two dipolar coupled nuclei including the nuclear Zeeman interactions has the following form:

$$\hat{H} = -\nu_1 \hat{l}_{1z} - \nu_2 \hat{l}_{2z} + H_{dip}, \quad (68)$$

where ν_1, ν_2 are the nuclear Larmor frequencies. If

$|\nu_1 - \nu_2| \gg \frac{\mu_0}{4\pi} \frac{\gamma_1 \gamma_2 \hbar}{r^3}$ then all non-diagonal terms in the Hamiltonian can be neglected:

$$\hat{H} = -\gamma_1 B_0 \hat{l}_{1z} - \gamma_2 B_0 \hat{l}_{2z} + \frac{\mu_0}{4\pi} \frac{\gamma_1 \gamma_2 \hbar}{r^3} (3 \cos^2 \theta - 1) \hat{l}_{1z} \hat{l}_{2z} = \quad (69)$$

$$= -\nu_1 m_1 - \nu_2 m_2 + \Delta m_1 m_2, \quad (70)$$

where $\Delta = \frac{\mu_0}{8\pi^2} \frac{\gamma_1 \gamma_2 \hbar}{r^3} (3 \cos^2 \theta - 1)$. The spectrum then would consist of two doublets centered around ν_1 and ν_2 and split by Δ .

3.1. Dipolar coupling Hamiltonian.

If $|\nu_1 - \nu_2| \sim \frac{\mu_0}{4\pi} \frac{\gamma_1 \gamma_2 \hbar}{r^3}$ then we need to include A and B terms, yielding a Hamiltonian:

$$\hat{H} = -\gamma_1 B_0 \hat{l}_{1z} - \gamma_2 B_0 \hat{l}_{1z} + \Delta (\hat{l}_{1z} \hat{l}_{1z} - \frac{1}{4} (\hat{l}_{1+} \hat{l}_{2-} + \hat{l}_{1-} \hat{l}_{2+})) \quad (71)$$

If $\nu_1 = \nu_2$ this Hamiltonian can be diagonalized in the singlet and triplet functions with their respective energies:

$$\begin{aligned} |s\rangle &= \frac{|\alpha\beta\rangle - |\beta\alpha\rangle}{\sqrt{2}} & E_s &= 0 \\ |t_1\rangle &= |\alpha\alpha\rangle & E_{t1} &= -\gamma B_0 - \frac{\Delta}{4} \\ |t_0\rangle &= \frac{|\alpha\beta\rangle + |\beta\alpha\rangle}{\sqrt{2}} & E_{t0} &= \frac{\Delta}{2} \\ |t_{-1}\rangle &= |\beta\beta\rangle & E_{t1} &= \gamma B_0 + \frac{\Delta}{4} \end{aligned} \quad (72)$$

3.1. Dipolar coupling Hamiltonian.

Problem

Which transitions are allowed? (Hint: use Eq.29)

3.1. Dipolar coupling Hamiltonian.

Problem

Which transitions are allowed? (Hint: use Eq.29)

Singlet and triplet functions have a total spin of 0 and 1 respectively. Introduce an operator of total spin $\hat{F} = \hat{\mathbf{l}}_1 + \hat{\mathbf{l}}_2$. Its eigenfunctions $|FM_F\rangle$ coincide with singlet ($F = 0$) and triplet ($F=1$) functions.

$F_+|FM_F\rangle = \sqrt{F(F+1) - M_F(M_F+1)}|FM_F+1\rangle$ operator can only change functions within one manifold, i.e a transition between singlet and triplet is forbidden. The only allowed transitions are in triplet manifold, changing $\delta M_F = \pm 1$. These are $|t_0\rangle \leftrightarrow |t_1\rangle$ and $|t_0\rangle \leftrightarrow |t_{-1}\rangle$.

3.1. Dipolar coupling Hamiltonian.

The transition frequencies are:

$$\begin{aligned}\nu_{0,1} &= \gamma B_0 - \frac{3}{4}\Delta \\ \nu_{0,-1} &= \gamma B_0 + \frac{3}{4}\Delta\end{aligned}\quad (73)$$

The two limiting cases were treated analytically and corresponding schematic spectra are shown in Fig.63.

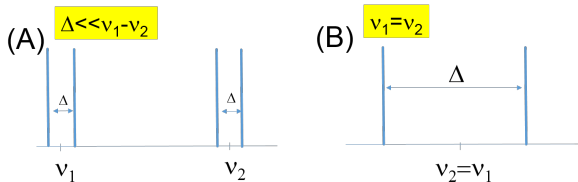


Fig.19: Schematic representation of single orientation spectra for (A) $|\nu_1 - \nu_2| \gg \Delta$ and (B) $\nu_1 = \nu_2$.

3.2. Powder spectra of dipolar coupled nuclei.

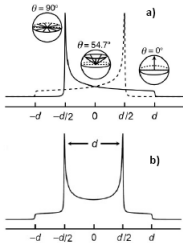


Fig.20: Powder pattern due to a pair of dipolar coupled spins (a) Dotted and continuous lines correspond to different transitions. Angles show related to continuous line. (b) Sum of contributions.

$$d = \frac{3\Delta}{2}$$

In most solids multiple spins interact via dipolar couplings, but in crystals of $\text{CaSO}_4 \cdot 2\text{H}_2\text{O}$ the water molecules are rather isolated from one another approximating an isolated pair. Studying the spectra as a function of crystal orientation help obtain orientational information.

In polycrystalline samples (powders) all values of θ will be simultaneously present and the spectrum is formed from a weighted superposition of the lines generated by the two transitions for all θ -values. The weighting related to the number of spin-pairs whose inter-nuclear vector takes a particular values of θ . This varies as $\sin \theta$ so that a "powder pattern" in the spectrum takes the form shown in Fig.64 .

3.2. Powder spectra of dipolar coupled nuclei.

The characteristic spectra shape is called "powder pattern". The two sharp features are called **Pake doublet**.

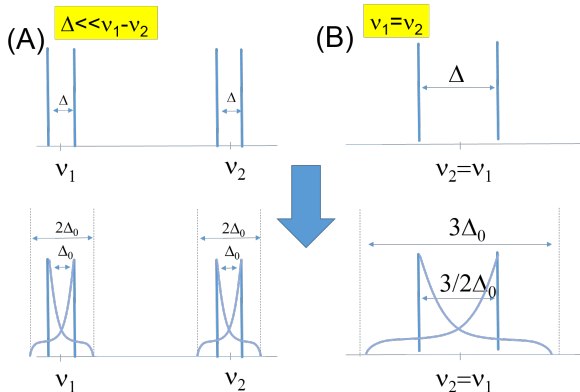


Fig.21: Schematic representation of polycrystalline spectra for (A) $|\nu_1 - \nu_2| \gg \Delta_0$, and (B) $\nu_1 = \nu_2$, where $\Delta_0 = \frac{\mu_0}{8\pi^2} \frac{\gamma_1 \gamma_2 \hbar}{r^3}$

3.3. Chemical shift anisotropy.

Raw NMR spectra from solids often form single broad peaks due to dipolar effects, along with the effects of chemical shift anisotropy, which often makes interpretation of spectra more complicated.

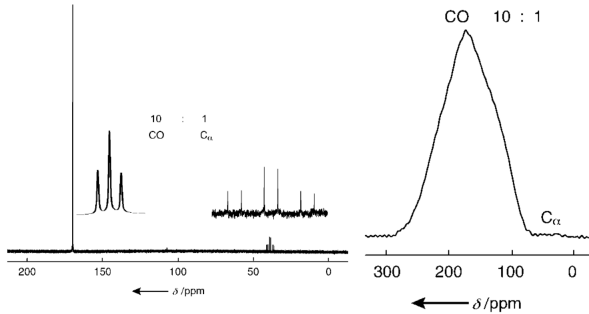


Fig.22: ^{13}C NMR spectrum of ^{13}C -labelled glycine: (a) 125 MHz solid state; (b) 75 MHz liquid state. From D.D. Laws, H.-M. Bitter, A.Jerschow., Angew. Chem. Int. Ed. 41, 3096 (2002)

3.3. Chemical shift anisotropy.

Chemical shift anisotropy results from the dependence of the level of shielding of a nucleus on the orientation of nearby bonds with respect to the magnetic field.

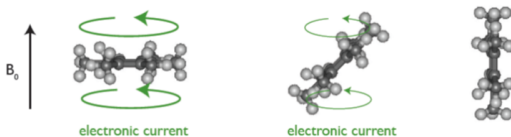


Fig.23: Dependence of shielding on the molecular orientation with respect to external magnetic field. (www.solidstatenmr.org.uk)

The effect is characterized by a shielding tensor which relates the induced shielding $\delta\mathbf{B}$ to the applied field B_0 taking into account the orientational dependence.

$$\begin{bmatrix} \delta B_x \\ \delta B_y \\ \delta B_z \end{bmatrix} = - \begin{bmatrix} \sigma_{xx} & \sigma_{xy} & \sigma_{xz} \\ \sigma_{yx} & \sigma_{yy} & \sigma_{yz} \\ \sigma_{zx} & \sigma_{zy} & \sigma_{zz} \end{bmatrix} \begin{bmatrix} 0 \\ 0 \\ B_0 \end{bmatrix} \quad (74)$$

This introduces a term in the Hamiltonian of the form,
 $\hat{H}_{CSA} = -\gamma(\delta\mathbf{B} \cdot \hat{\mathbf{I}})$.

3.3. Chemical shift anisotropy.

In secular approximation, when the nuclear Zeeman interaction $\gamma B_0 \gg \gamma \sigma_{i,j} B_0$, which is why the secular spin Hamiltonian is truncated to:

$$\hat{H}_{CSA} = \gamma \sigma_{zz} B_0 \quad (75)$$

In the laboratory frame in order σ_{zz} component can be found from a full tensor using a product with a unit vector along the direction of B_0 :

$$\sigma_{zz}^{lab} = [0 \ 0 \ 1] \begin{bmatrix} \sigma_{xx} & \sigma_{xy} & \sigma_{xz} \\ \sigma_{yx} & \sigma_{yy} & \sigma_{yz} \\ \sigma_{zx} & \sigma_{zy} & \sigma_{zz} \end{bmatrix} \begin{bmatrix} 0 \\ 0 \\ 1 \end{bmatrix} = \mathbf{b}_0^T \boldsymbol{\sigma} \mathbf{b}_0 \quad (76)$$

3.3. Chemical shift anisotropy.

In the principle axis system the tensor has the following form:

$$\boldsymbol{\sigma} = \begin{bmatrix} \sigma_1 & 0 & 0 \\ 0 & \sigma_2 & 0 \\ 0 & 0 & \sigma_3 \end{bmatrix} \quad (77)$$

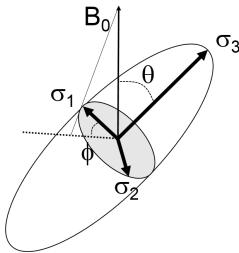


Fig.24: Schematic representation of CSA tensor components.

The expression for σ_{zz}^{lab} in Eq.76 is a true scalar, i.e. it does not depend in which reference frame it is written. We can write it in the principle axis system of the tensor, where the direction of magnetic field is $\mathbf{b}_{PAS} = [\sin \theta \cos \phi, \sin \theta \sin \phi, \cos \theta]$.

$$\sigma_z z^{lab} = \mathbf{b}_0^T \boldsymbol{\sigma}^{lab} \mathbf{b}_0 = \mathbf{b}_{PAS}^T \boldsymbol{\sigma}^{PAS} \mathbf{b}_{PAS} = \quad (78)$$

$$= \sigma_1 \sin^2 \theta \cos^2 \phi + \sigma_2 \sin^2 \theta \sin^2 \phi + \sigma_3 \cos^2 \theta \quad (79)$$

3.3. Chemical shift anisotropy.

PAS axis are usually chosen such that σ_3 component is the largest.
We can use a more convenient notation, by replacing:

$$\sigma_{iso} = \frac{\sigma_1 + \sigma_2 + \sigma_3}{3} - \text{isotropic chemical shift} \quad (80)$$

$$\Delta = \sigma_3 - \sigma_{iso} - \text{anisotropy} \quad (81)$$

$$\eta = \frac{\sigma_1 - \sigma_2}{\sigma_3} - \text{asymmetry} \quad (82)$$

Using this notation the σ_{zz}^{lab} can be found using a compact equation:

$$\sigma_{zz}^{lab} = \sigma_{iso} + \frac{\Delta}{2}(3 \cos^2 \theta - 1 + \eta \sin^2 \theta \cos 2\phi) \quad (83)$$

3.3. Chemical shift anisotropy.

$$\sigma_{zz}^{lab} = \sigma_{iso} + \frac{\Delta}{2}(3\cos^2\theta - 1 + \eta\sin^2\theta\cos 2\phi)$$

Spectra of polycrystalline samples would produce broad patterns shown in Fig.71

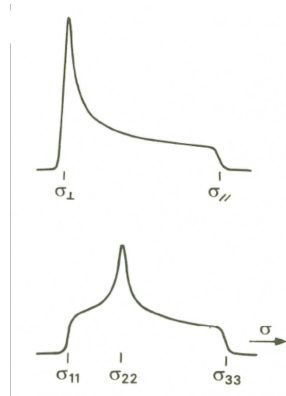


Fig.25: Powder patterns for (a) $\sigma_1 = \sigma_2 = \sigma_{\perp}, \sigma_3 = \sigma_{\parallel}$, (b) $\sigma_1 \neq \sigma_2 \neq \sigma_3$

Summary of Lecture 5.

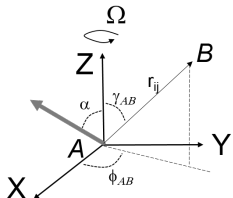
- Spin magnetic moments interact via dipolar interaction
- Spectra of dipolar coupled spins are anisotropic
- Chemical shift is anisotropic as well

Suggested reading: Harris 6.6, 6.7, 4.1, 4.2, Slichter 3.1

3.4. Magic angle spinning.

How can we make the spectra simpler? Magic angle spinning is a technique where the sample is rapidly spun around the axis tilted with respect to 54.5 deg with respect to magnetic field. It allows to removing (almost) all anisotropy arising from the dipolar and CSA interactions. For instance, for dipolar interaction consider two nuclei A and B . Place the beginning of coordinates at A , Z -axis is pointed along the rotation axis and choose X , Y -axis such that magnetic field \mathbf{B} is in xz -plane $\mathbf{B} = B_0 [\sin \alpha, 0, \cos \alpha]$. The radius-vector connecting the two nuclei:

$$\mathbf{r}_{AB} = r_{AB} [\sin \gamma_{AB} \cos \phi_{AB}, \sin \gamma_{AB} \phi_{AB}, \cos \gamma_{AB}] \quad (84)$$



3.4. Magic angle spinning.

Since the sample is spinning, then:

$$\phi_{AB} = \phi_{AB}^0 + \Omega t, \quad (85)$$

where ϕ_{AB}^0 is some initial phase. We are interested averaging of $(1 - 3\cos^2 \theta_{AB})$. Since:

$$\cos \theta_{AB} = \frac{(\mathbf{r}_{AB} \cdot \mathbf{B})}{r_{AB} B_0} = \sin \gamma_{AB} \cos \phi_{AB} \sin \alpha + \cos \gamma_{AB} \cos \alpha \quad (86)$$

then:

$$1 - 3\cos^2 \theta = 1 - 3\sin^2 \gamma_{AB} \cos^2 \phi_{AB} \sin^2 \alpha - 3\cos^2 \gamma_{AB} \cos^2 \alpha - \quad (87)$$

$$- 6 \sin \gamma_{AB} \cos \phi_{AB} \sin \alpha \cos \gamma_{AB} \cos \alpha \quad (88)$$

For phases linearly varying with time $\overline{\cos \phi_{AB}} = 0$, $\overline{\cos^2 \phi_{AB}} = \frac{1}{2}$, therefore:

3.4. Magic angle spinning.

For phases linearly varying with time $\overline{\cos \phi_{AB}} = 0$, $\overline{\cos^2 \phi_{AB}} = \frac{1}{2}$, therefore:

$$\overline{1 - 3 \cos^2 \theta_{AB}} = -\frac{1}{2}(1 - 3 \cos^2 \alpha)(1 - 3 \cos^2 \gamma_{AB}) \quad (89)$$

When α is to the "magic angle" of $\theta_m = 54.7$ deg, $\cos^2 \theta_m = \frac{1}{3}$ and the expression in Eq.89 is zero and independent on γ_{AB} . It means the dipolar interaction is averaged to zero and it does not show up in the spectrum. So if the spinning is fast enough (i.e. $\Omega \gg \frac{\gamma_1 \gamma_2 \hbar}{r^3}$ or $\gamma \sigma_{max} B_0$) instead of wide lines due to CSA or dipolar only sharp lines (liquid-state like) spectrum arises.

3.4. Magic angle spinning.

The technique of sample spinning under the angle of $\theta_m = 54.7$ deg is called **Magic Angle Spinning**.

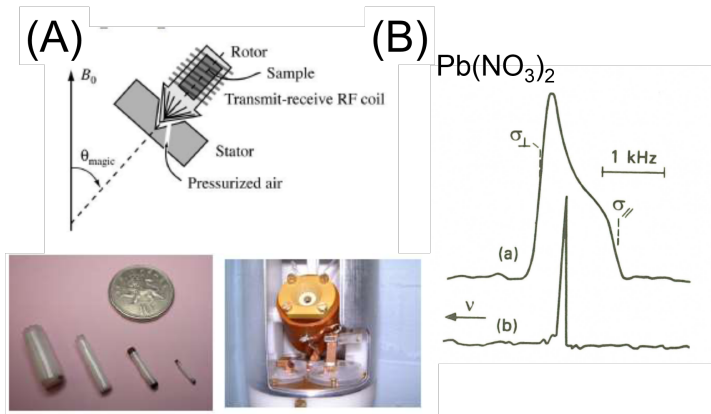
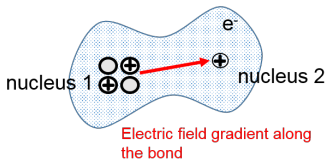


Fig.26: (A) MAS rotors (B) NMR spectrum of ^{207}Pb in lead nitrate under static and MAS conditions.

3.5. Quadrupolar interaction.

All nuclei with a spin greater than $\frac{1}{2}$ have an electric quadrupole moment. Electric quadrupoles interact with electric field gradients. In atoms and molecules the electrons and nuclei create electric fields (and electric field gradients) at the location of a nucleus.



Quadrupolar moment is a tensor and is proportional to a tensor combined of spin components (Wigner-Eckart theorem). The quadrupolar coupling Hamiltonian is:

$$\hat{H}_Q = \frac{eQ}{6I(2I-1)\hbar} \sum_{i,j=x,y,z} \hat{l}_i e q_{ij} \hat{l}_j, \quad (90)$$

where eQ is a quadrupole moment, a constant depends only on a nuclear species, eq_{ij} are the components of electric field gradient tensor.

3.5. Quadrupolar interaction.

The quadrupolar interaction tensor is traceless, i.e. has only two independent components. If its principal components are defined as q_{xx}^{PAS} , q_{yy}^{PAS} , q_{zz}^{PAS} , then two parameters describing the tensor can be introduced:

$$\chi = \frac{e^2 q_{zz}^{PAS} Q}{\hbar} \text{-quadrupole coupling constant} \quad (91)$$

$$\eta_Q = \frac{q_{xx}^{PAS} - q_{yy}^{PAS}}{q_{zz}^{PAS}} \text{-asymmetry parameter} \quad (92)$$

In the PAS the hamiltonian has a form:

$$\hat{H}_Q = \frac{\chi}{4I(2I-1)} \left(3\hat{I}_z^2 - I(I+1) + \eta_Q (\hat{I}_x^2 - \hat{I}_y^2) \right) \quad (93)$$

3.5. Quadrupolar interaction.

In case of axial symmetry, $\eta_Q = 0$, the Hamiltonian of a quadrupolar nucleus in the magnetic field:

$$\hat{H} = -\nu_0 \hat{I}_z + \frac{\chi}{8} (3 \cos^2 \theta - 1) \frac{3\hat{I}_z^2 - I(I+1)}{I(2I-1)}, \quad (94)$$

where θ is the direction of the magnetic field in the PAS of quadrupolar tensor. Since the selection rule is $\Delta m_I = \pm 1$ the transition frequencies are:

$$\nu = \nu_0 - \frac{3}{8} \chi \frac{2m_I - 1}{I(2I-1)} (3 \cos^2 \theta - 1) \quad (95)$$

3.5. Quadrupolar interaction.

$$\nu = \nu_0 - \frac{3}{8} \chi \frac{2m_I - 1}{I(2I-1)} (3\cos^2 \theta - 1) \quad (96)$$

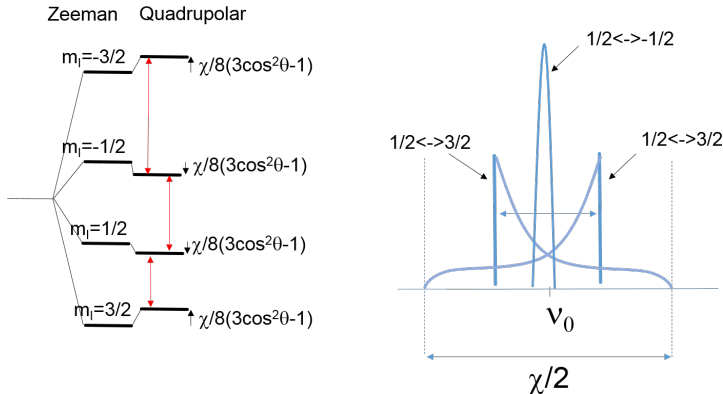


Fig.27: (A) Level diagram for $I = \frac{3}{2}$ nucleus, (B) Schematic representation of its spectrum in a polycrystalline sample

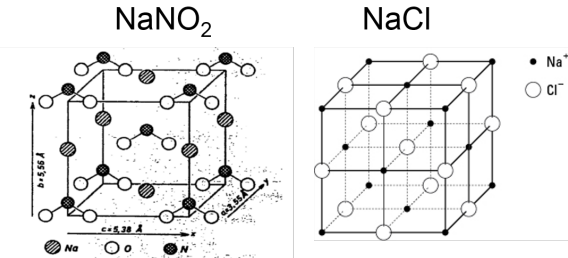
3.5. Quadrupolar interaction.

The magnitude of quadrupolar coupling could be rather large (up to 1000 MHz). Even for the same nucleus in different chemical environment could have very different quadrupolar coupling, because the electric field gradient might be very different.

$$\hat{H}_Q = \frac{eQ}{6I(2I-1)\hbar} \sum_{i,j=x,y,z} \hat{l}_i e q_{ij} \hat{l}_j, \quad (97)$$

Problem

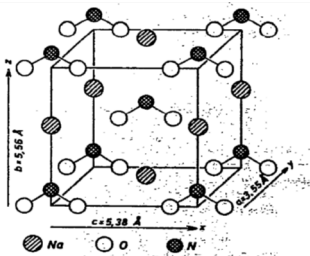
Which Na quadrupolar coupling is larger: in NaCl or NaNO_2 crystals?



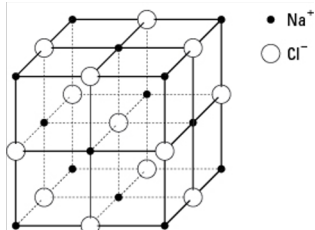
Answer

NaCl crystals have very high cubic symmetry, and electric field gradient at the location of Na is zero. While in NaNO_2 crystal the electric field gradient is not zero due to the shape of NO_2 , $\chi \approx 1.1$ MHz.

NaNO_2



NaCl

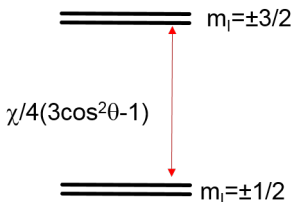


3.5. Quadrupolar interaction.

$$\nu = \nu_0 - \frac{3}{8}\chi \frac{2m_I - 1}{I(2I - 1)} (3\cos^2 \theta - 1) \quad (98)$$

In principle, the transitions between sublevels of quadrupolar nuclei can be observed even at zero magnetic field. The technique for this is called **Nuclear Quadrupolar Resonance**.

Zero magnetic field



Summary of Lecture 6.

- Magic Angle Spinning removes most of anisotropy of dipolar, CSA and quadrupolar coupling.
- Quadrupolar coupling emerges due to interaction of quadrupolar moment with electric field gradient
- Spectra of quadrupolar nuclei in solids are anisotropic
- Strength of electric field gradient matters (symmetric environment is better)
- Sometimes no magnetic field is needed to observe transitions in a spin system.

Suggested reading: Harris Appendix 5,
ch.5.9,5.10,5.11,5.12,5.13, Slichter 3.1, for more detailed
explanation of origins of the quadrupolar coupling - Slichter ch 10.
In addition "Solid-state NMR Spectroscopy Principles and
Applications" by M. Duer: Ch 1.4 "Nuclear spin interactions".

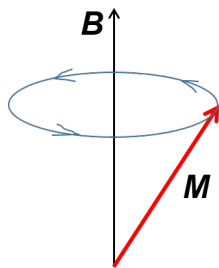
Spin dynamics.

- Rotating frame.
- Detection of NMR signals.
- Relaxation and Bloch equations
- Spin echo

4.1. Rotating frame.

Let's recall the solution for the equations of motion of a magnetic moment:

In a uniform magnetic field directed along z -axis $\mathbf{B} = (0, 0, B_0)$, the equation for individual components of \mathbf{M} follow the equations:



$$\begin{aligned}\frac{dM_x}{dt} &= \omega_L M_y \\ \frac{dM_y}{dt} &= -\omega_L M_x \\ \frac{dM_z}{dt} &= 0,\end{aligned}\quad (99)$$

where $\omega_L = \gamma B_0$ - Larmor frequency.

A solution to this system of differential equations with initial values of $M_x(0)$, $M_y(0)$, $M_z(0)$ has the following form:

$$\begin{aligned}M_x(t) &= M_x(0) \cos(\omega_L t) + M_y(0) \sin(\omega_L t) \\ M_y(t) &= -M_y(0) \sin(\omega_L t) + M_y(0) \cos(\omega_L t) \\ M_z(t) &= M_z(0)\end{aligned}\quad (100)$$

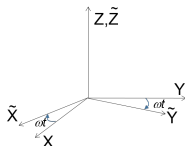
4.1. Rotating frame.

Let's explore, how oscillating transverse magnetic fields affect the evolution of a magnetic moment. This can be done by recording the equations for magnetization in the **rotating frame**.

Now we want to transform these equations into a frame which rotates at the angular velocity ω . The coordinates in the laboratory frame (x, y, z) can be expressed through the coordinates of the lefthand-rotating frame $(\tilde{x}, \tilde{y}, \tilde{z})$, shown schematically in Fig.29:

$$\begin{aligned} x &= \tilde{x} \cos \omega t + \tilde{y} \sin \omega t \\ y &= -\tilde{x} \sin \omega t + \tilde{y} \cos \omega t \\ z &= \tilde{z} \end{aligned} \tag{101}$$

Fig.28: Rotating frame coordinates $(\tilde{x}, \tilde{y}, \tilde{z})$ with respect to laboratory frame coordinates (x, y, z) .



4.1. Rotating frame.

For a point $(\tilde{x}, \tilde{y}, \tilde{z})$ stationary in the rotating frame, the time change of the laboratory frame coordinates becomes:

$$\begin{aligned}\frac{dx}{dt} &= \omega y \\ \frac{dy}{dt} &= -\omega x \\ \frac{dz}{dt} &= 0\end{aligned}\tag{102}$$

For any vector \mathbf{a} stationary in the rotating frame Eqs.102 can be rewritten in a compact form:

$$\frac{d\mathbf{a}}{dt} = \boldsymbol{\Omega} \times \mathbf{a},\tag{103}$$

where $\boldsymbol{\Omega} = (0, 0, -\omega)$ is an angular velocity vector.

4.1. Rotating frame.

Magnetization vector \mathbf{M} in the laboratory frame can be represented as a sum of its individual components along the main axis of the rotating frame $\mathbf{M} = \tilde{M}_x \tilde{\mathbf{e}}_x + \tilde{M}_y \tilde{\mathbf{e}}_y + \tilde{M}_z \tilde{\mathbf{e}}_z$. The time derivative for such a vector can then be calculated as:

$$\begin{aligned}\frac{d\mathbf{M}}{dt} &= \frac{d\tilde{M}_x}{dt} \tilde{\mathbf{e}}_x + \tilde{M}_x \frac{d\tilde{\mathbf{e}}_x}{dt} + \frac{d\tilde{M}_y}{dt} \tilde{\mathbf{e}}_y + \tilde{M}_y \frac{d\tilde{\mathbf{e}}_y}{dt} + \frac{d\tilde{M}_z}{dt} \tilde{\mathbf{e}}_z + \tilde{M}_z \frac{d\tilde{\mathbf{e}}_z}{dt} = \\ &= \frac{\delta \mathbf{M}}{\delta t} + \boldsymbol{\Omega} \times \mathbf{M}\end{aligned}, \quad (104)$$

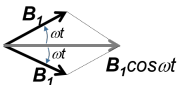
where symbol $\frac{\delta \mathbf{M}}{\delta t}$ represents a change of magnetization with respect to rotating frame unit vectors $\tilde{\mathbf{e}}_x, \tilde{\mathbf{e}}_y, \tilde{\mathbf{e}}_z$. Recalling equation describing precession Eq.7 $\frac{\delta \mathbf{M}}{\delta t}$ can be expressed as:

$$\frac{\delta \mathbf{M}}{\delta t} = \frac{d\mathbf{M}}{dt} - \boldsymbol{\Omega} \times \mathbf{M} = \gamma \mathbf{M} \times \mathbf{H} + \mathbf{M} \times \boldsymbol{\Omega} = \gamma \mathbf{M} \times \mathbf{B}_{\text{eff}}, \quad (105)$$

where $\mathbf{B}_{\text{eff}} = \mathbf{B}_0 + \frac{\boldsymbol{\Omega}}{\gamma}$ is an effective magnetic field.

4.1. Rotating frame.

Fig.29: Oscillating field decomposed into two components, where one rotates clockwise and the other counterclockwise.



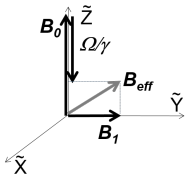
The magnetic field oscillating at frequency ω can be represented as two fields rotating clockwise and anti-clockwise

$$2B_1 \cos \omega t = B_1 \exp(i\omega t) + \exp(-i\omega t) \quad (106)$$

shown schematically in Fig.29B.

4.1. Rotating frame.

Fig.30: Schematic representation of effective field B_{eff} in the rotating frame.



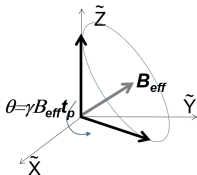
In the frame rotating left, the effective magnetic field then becomes:

$$B_{\text{eff}} = B_0 + \frac{\Omega}{\gamma} + B_1 \quad (107)$$

where terms associated with the right rotation are discarded, because the oscillate at a very high frequency 2ω in the left rotating frame and have little effect.

4.1. Rotating frame.

Fig.31: Action of a pulse on the magnetization vector M .



Magnetization in the rotating frame precesses with its respective Larmor frequency around the direction of an effective magnetic field \mathbf{H}_{eff} given by Eq.107. For a field oscillating on resonance (i.e. exactly at the Larmor frequency) the effective field has components only along x, y -axis. If the oscillating magnetic field is applied for a brief period of time t_p , i.e. in a form of a pulse, the effect of such a pulse is a rotation of magnetization by a finite angle:

$$\theta = \gamma B_1 t_p \quad (108)$$

4.1. Rotating frame.

The evolution of magnetization is more complex when viewed in the laboratory frame as it involves precession about both applied fields (B_0 and B_{eff}). If a 90° on-resonance pulse ($\gamma B_0 t_p = \frac{\pi}{2}$) is applied the magnetization is rotated to point along the y-axis in the rotating frame. If the pulse duration is such that $\gamma B_0 t_p = \frac{\pi}{2}$ (a 180° RF pulse) the magnetization is rotated to point along the z-axis.

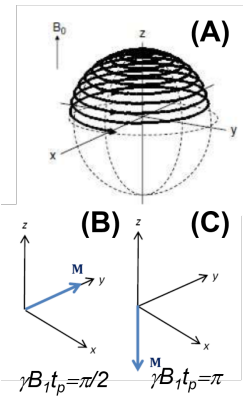


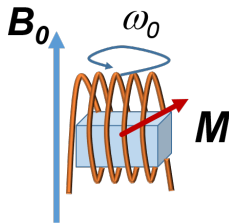
Fig.32: (A) Evolution of magnetization in the laboratory frame; (B) Magnetization in the rotating frames immediately after a 90° pulse and (C) 180°

4.2. Detection of NMR signals.

After a 90° RF pulse the equilibrium magnetization has been rotated into the transverse (x, y)-plane, and will then precess about the z -axis in the laboratory frame at the Larmor frequency, $\omega = \gamma B_0$ (but remains stationary in the rotating frame).

The precessing magnetization generates a magnetic field which varies sinusoidally with time at the Larmor frequency. The field will induce a voltage in a nearby coil, by electromagnetic induction. The resulting voltage also varies sinusoidally with time at the Larmor frequency. The voltage is the NMR signal that we measure.

Fig.33: A sample with magnetization M placed inside a coil.



4.2. Detection of NMR signals.

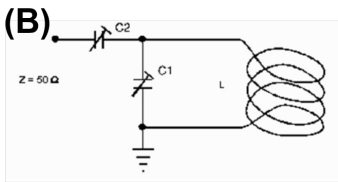
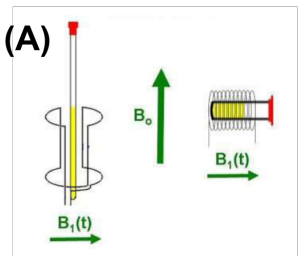


Fig.34: (A) Saddle and solenoidal RF coils (B) The RF coil with inductance L is tuned (with capacitor, C_1) to resonate at frequency ω_0) and is matched to an impedance of 50Ω) (with capacitor C_2) (C) A photograph of a solution NMR probe

4.3. Relaxation and Bloch equations

Let's recall the equations guiding the motion of magnetization vector:

$$\begin{aligned}\frac{dM_x}{dt} &= \omega_L M_y \\ \frac{dM_y}{dt} &= -\omega_L M_x \\ \frac{dM_z}{dt} &= 0,\end{aligned}\tag{109}$$

where $\omega_L = \gamma B_0$ - Larmor frequency. They can be modified to include relaxation terms:

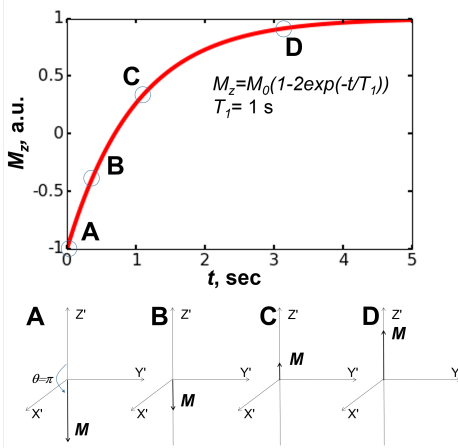
$$\begin{aligned}\frac{dM_x}{dt} &= \omega_L M_y - \frac{M_x}{T_2} \\ \frac{dM_y}{dt} &= -\omega_L M_x - \frac{M_y}{T_2} \\ \frac{dM_z}{dt} &= -\frac{M_z - M_0}{T_1},\end{aligned}\tag{110}$$

where T_1, T_2 - are time constants called longitudinal and transverse relaxation times respectively. We dealt with T_1 earlier.

4.3. Relaxation and Bloch equations

If we consider the evolution of magnetization in the absence of RF, then for longitudinal magnetization M_z we obtain a solution:

$$M_z(t) = M_0 - (M_0 - M_z(0))e^{-t/T_1} \quad (111)$$



4.3. Relaxation and Bloch equations

The transverse magnetization has a solution:

$$\begin{aligned} M_x(t) &= (M_x(0) \cos(\omega t) + M_y(0) \sin(\omega t)) e^{t/T_2} \\ M_y(t) &= (M_y(0) \cos(\omega t) - M_x(0) \sin(\omega t)) e^{t/T_2} \end{aligned} \quad (112)$$

Problem

For the initial $M_x(0) = 1$, $M_y(0) = 0$ consider the signal $S(t) \sim \cos(\omega t)e^{t/T_2} + i \sin(\omega t)e^{t/T_2}$. Find its Fourier Transform with respect to time.

4.3. Relaxation and Bloch equations

Eqs.112 describe magnetization following a $\frac{\pi}{2}$ pulse, the magnetization following this pulse is called **free induction decay (FID)** and is being recorded by the NMR spectrometer.

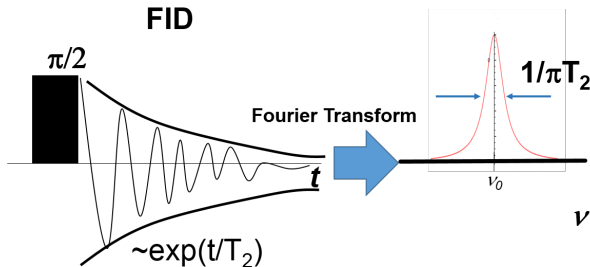


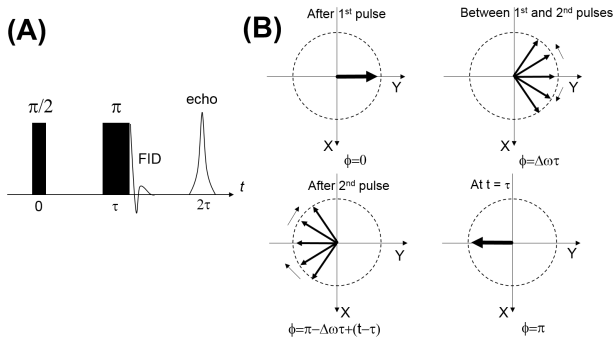
Fig.35: NMR spectra are produced by taking a Fourier transform from the detected FID.

4.3. Relaxation and Bloch equations

T_2 relaxation is responsible for so called **homogeneous** broadening of NMR line. Previously we have seen examples of **inhomogeneous** broadening, where the line has a complex pattern, due to a CSA, dipolar or quadrupolar interaction. After an applied $\pi/2$ pulse the magnetization dephases due to differences in precession frequencies, however, there is a way to refocus it.

4.4. Spin echo

Consider magnetization in the rotating frame. After a $\pi/2$ pulse the magnetization is rotated into X , Y -plane and then it dephases due to differences in precession frequencies in different molecules. At the moment τ a π -pulse instantaneously changes the phases of magnetization vectors. In the next interval they continue precessing with their respective frequencies and refocus at $t = 2\tau$.



Summary of Lecture 7.

- Rotating frame frame is a very useful formalism allowing to simplify the time-evolution of magnetization under the action of pulses
- NMR signals are detected by measuring the voltages induced by the samples in the coil
- Bloch equations phenomenologically describe dissipation processes
- Spin echo is observed in the a simple two-pulse sequence

Suggested reading: Harris 3.1, 3.2, 3.3, 3.7, 3.8, 3.13, Slichter Ch. 2 for the quantum mechanical treatment of rotating frame and spin echos.

NMR Relaxation Mechanisms

- T_1 relaxation
- T_2 relaxation
- Relaxation mechanisms.

5.1. T_1 relaxation

NMR relaxation is driven by temporal fluctuations of the terms in the spin Hamiltonian:

$$\hat{H}_{\text{spin}} = \hat{H}_Z + \hat{H}_{CS} + \hat{H}_J + \hat{H}_{\text{dip}} + \hat{H}_Q, \quad (113)$$

usually resulting from molecular motion. Variations in non-secular terms of the Hamiltonian drive T_1 -relaxation, since these cause transitions between the Zeeman eigenstates, while variations in the secular terms do not. Fluctuations in the secular terms do drive T_2 relaxation. The non-secular terms also contribute to T_2 relaxation. These effects can in some cases relate to fluctuations of the magnetic fields experienced by the nuclear spins (e.g. due to variation in the dipolar fields produced by one nuclear magnetic moment at the site of another or due to variation in shielding, both resulting from molecular motion). Here, we will first see how the transition rates in a simple system of isolated spins can be related to the T_1 relaxation time and then establish the rate of transitions generated by randomly fluctuating magnetic fields.

5.1. T_1 relaxation

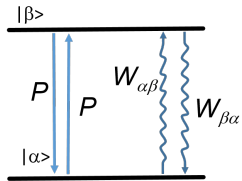
To gain some insight, we now consider the effect of a fluctuating magnetic field, $\mathbf{B}_L(t)$ initially focusing on the effect of the x -component, which can be written as:

$$\mathbf{B}_L(t) = B_{xL}f(t), \quad (114)$$

where $f(t)$ is a randomly varying function, such that $\overline{f(t)} = 0$ and $\overline{f(t)^2} = 1$, and B_{xL} characterizes the amplitude of the fluctuating field. This introduces a time-dependent term in the Hamiltonian of the form:

$$\hat{V}(t) = -\gamma \hat{I}_x B_{xL} f(t) \quad (115)$$

5.1. T_1 relaxation



Previously we considered a two-level system (see section 9), where we introduced the rate of spontaneous transitions

$W = \frac{1}{2}(W_{12} - W_{21})$ and found that **longitudinal = spin-lattice**:

$$T_1 = \frac{1}{2W} \quad (116)$$

The rate W can be calculated based using $V(t)$ as a perturbation (see Harris Appendix 3).

5.1. T_1 relaxation

This gives the transition rate from state $|1\rangle \rightarrow |2\rangle$ as:

$$\begin{aligned} W &= \int_{-\infty}^{\infty} \overline{\langle 1 | \hat{V}(t+\tau) | 2 \rangle \langle 2 | \hat{V}(t) | 1 \rangle} e^{-i\omega\tau} d\tau = \\ &= (\gamma B_{xL})^2 |\langle 2 | \hat{I}_x | 1 \rangle|^2 \int_{-\infty}^{\infty} \overline{f(t+\tau)f(t)} e^{-i\omega\tau} d\tau \quad (117) \end{aligned}$$

Here the over-bar means "average" = average over the ensemble of spins in the sample. Recognising that $|1\rangle = |\alpha\rangle$ and $|2\rangle = |\beta\rangle$ and $\langle | \hat{I}_x | \rangle = \frac{1}{2}$, this gives:

$$W = \frac{(\gamma B_{xL})^2}{4} \int_{-\infty}^{\infty} \overline{f(t+\tau)f(t)} e^{-i\omega_0\tau} = \frac{(\gamma B_{xL})^2}{4} J(\omega_0), \quad (118)$$

where $G(\tau) = \overline{f(t+\tau)f(t)}$ is the **auto-correlation** of $f(t)$ and $J(\omega)$ is the **spectral density**, which form a Fourier transform pair with the auto-correlation function.

5.1. T_1 relaxation

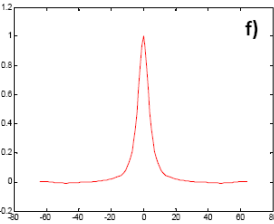
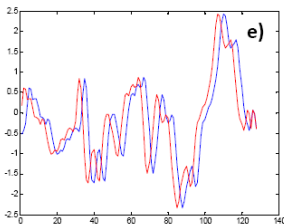
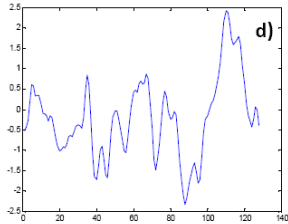
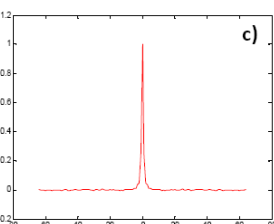
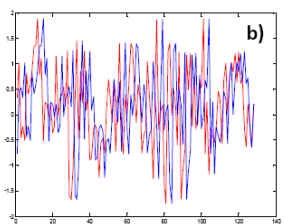
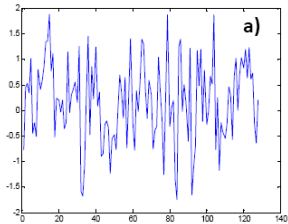
The auto-correlation function $G(\tau)$ is found by shifting the function $f(t)$ in time by an amount τ , to form $f(t + \tau)$, then multiplying this by the original function and forming the average of the resulting product over spins in the ensemble (all experiencing different varying fields). The result is independent of t , but depends on τ .

$G(\tau)$ takes a value of 1 for $\tau = 0$ and decreases monotonically to zero as τ increases. The time-span over which $G(\tau)$ decays is linked to the correlation time, τ_c which characterizes the time that it takes for the field experienced by each nucleus to change significantly. A rapidly fluctuating field gives rise to a narrower correlation function.

5.1. T_1 relaxation

Let's take a closer look at **autocorrelation function**:

$$G(\tau) = \overline{f(t + \tau)f(t)}$$



5.1. T_1 relaxation

The Fourier transfer of the auto-correlation function is the **spectral density**, $J(\omega)$, which characterizes the variation of the "power" of fluctuations with frequency. Reducing the correlation time, increases the range of frequencies spanned by the power spectrum. If we also consider the effect of the fluctuating y -component of the field, this generates a similar contribution to W , since $B_{xL} = B_{yL}$ and $|\langle 2 | \hat{I}_x | 1 \rangle|^2 = |\langle 2 | \hat{I}_y | 1 \rangle|^2 = \frac{1}{4}$. However, the fluctuating z -component does not contribute, since $|\langle 2 | \hat{I}_z | 1 \rangle|^2 = 0$.

$$\text{Consequently, } \frac{1}{T_1} = 2W = (\gamma B_{xL})^2 J(\omega)$$

5.1. T_1 relaxation

For fluctuations related to molecular rotation, the autocorrelation function is generally well described by:

$$G(\tau) = e^{-\frac{|\tau|}{\tau_c}}, \quad (119)$$

where τ_c is the correlation time, which decreases as the temperature increases as a result of increased thermal motion. Fourier transformation of $G(\tau)$ gives:

$$J(\omega) = \frac{2\tau_c}{1 + \omega^2\tau_c^2} \quad (120)$$

5.1. T_1 relaxation

Spectral density for a random process with exponential correlation function:

$$J(\omega) = \frac{2\tau_c}{1 + \omega^2\tau_c^2}$$

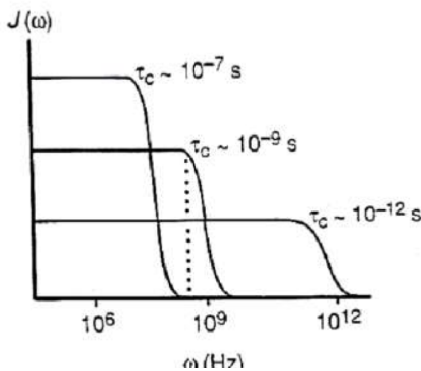


Fig.36: Spectral density for exponential autocorrelation function.

5.1. T_1 relaxation

The rate of T_1 -relaxation due to fluctuations of the field is then given by:

$$\frac{1}{T_1} = (\gamma B_{xL})^2 \frac{2\tau_c}{1 + \omega^2 \tau_c^2} \quad (121)$$

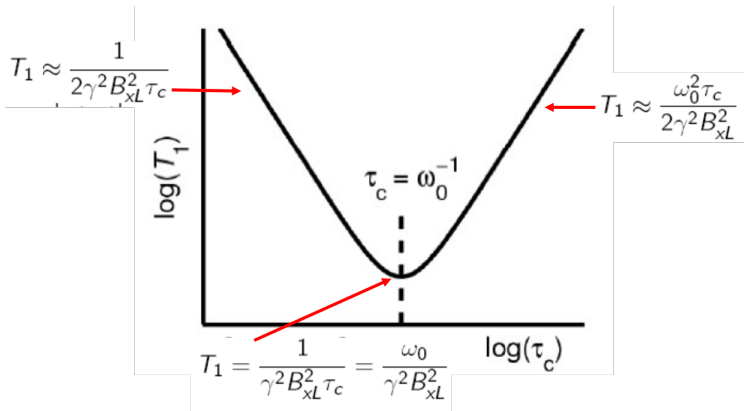


Fig.37: T_1 variation with correlation time in a log-log plot.

5.1. T_1 relaxation

The value of T_1 depends on the size of τ_c versus ω^{-1} . Under conditions of rapid motion $\omega_0\tau_c \ll 1$, $T_1 \approx \frac{1}{2\gamma^2 B_{xL}^2 \tau_c}$, thus increasing as τ_c decreases. This corresponds to the **extreme line narrowing condition**, which hold for small molecules (e.g. $\tau_c \sim 2$ ps for water and if $\frac{\omega_0}{2\pi} = 400$ MHz at 9.4 T, then $\omega_0\tau_2 \approx 0.005$) In contrast, when the motion is slow $\omega_0\tau_c \gg 1$, $T_1 \approx \frac{\omega_0^2 \tau_c}{2\gamma^2 B_{xL}^2}$ and T_1 increase as the correlation time increases (corresponding to decreasing temperature). The minimum of T_1 occurs when $\omega_0\tau_c \sim 1$, where the fluctuations at the Larmor frequency are the largest. This gives a minimum T_1 values of

$$T_1 = \frac{1}{\gamma^2 B_{xL}^2 \tau_c} = \frac{\omega_0}{\gamma^2 B_{xL}^2}$$

5.2. T_2 relaxation

Following a similar analysis, it can be shown that the effect of local field fluctuations on T_2 relaxation is described by:

$$\frac{1}{T_2} = \frac{(\gamma B_{xL})^2}{2} J(\omega_0) + \frac{(\gamma B_{zL})^2}{2} J(0) = \frac{1}{2 T_1} + (\gamma B_{xL})^2 \tau_c \quad (122)$$

In the extreme narrowing limit, assuming field fluctuations in all directions are of similar magnitude (i.e. $B_{zL} = B_{xL} = B_{yL}$), this gives $T_2 = T_1$.

As the correlation time increases, the contribution of the $J(0)$ term becomes increasingly important and T_2 thus becomes shorter than T_1 (e.g. for large macromolecules).

5.2. T_2 relaxation

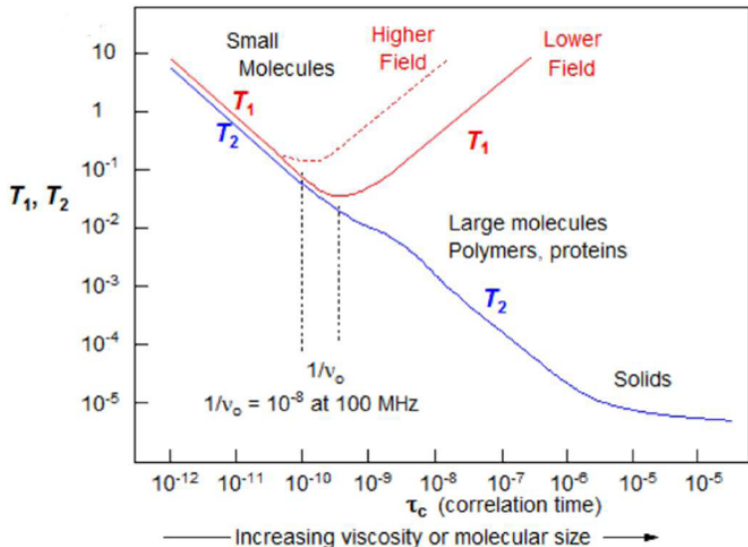


Fig.38: Variation of T_1 and T_2 with correlation time τ (log-log plot) Source: <http://www.chem.wisc.edu/areas/reich/nmr>

5.3. Relaxation mechanisms.

The rate of relaxation depends on the square of the size of the effective field fluctuations. Table below lists expressions for the relaxation rate $\frac{1}{T_1}$ in the extreme narrowing limit for a variety of different mechanisms.

Table 3-2 Equations for spin-lattice relaxation rates, T_1^{-1} , of a spin- $\frac{1}{2}$ nucleus, A, for various mechanisms in the extreme narrowing approximation

Mechanism	T_1^{-1}	Notes
dd(intra)(homo)	$\left(\frac{\mu_0}{4\pi}\right)^2 \frac{3}{2} \gamma_A^4 \hbar^2 \tau_c / r^6$	for a single pair of spin- $\frac{1}{2}$ nuclei of separation r
dd(intra)(hetero)	$\left(\frac{\mu_0}{4\pi}\right)^2 \frac{4}{3} \gamma_A^2 \gamma_X^2 \hbar^2 \tau_c / r^6$	for a single pair of spin- $\frac{1}{2}$ nuclei AX of separation r
dd(inter)(hetero)	$\left(\frac{\mu_0}{4\pi}\right)^2 \frac{2}{15} N_X \gamma_A^2 \gamma_X^2 \hbar^2 / D_a$	for relaxation by a spin- $\frac{1}{2}$ nucleus X
ue(intra)(dipolar)	$\left(\frac{\mu_0}{4\pi}\right)^2 \frac{4}{3} \gamma_A^2 \gamma_e^2 \hbar^2 S(S+1) \tau_c / r^6$	for relaxation by unpaired electrons of total spin S at distance r
ue(scalar)	$\frac{8}{3} \pi^2 a_N^2 S(S+1) \tau_e$	for relaxation by unpaired electrons of total spin S
sr	$2I_a k T C^2 \tau_{sr} / \hbar^2$	for isotropic molecular inertia
sa	$\frac{2}{15} \gamma_A^2 B_0^2 \Delta \sigma^2 \tau_c$	for cylindrical symmetry of shielding
sc	$\frac{8}{3} \pi^2 J_{AX}^2 I_X (I_X + 1) \frac{\tau_{sc}}{1 + (\omega_X - \omega_A)^2 \tau_{sc}^2}$	relaxation by coupling to spin, X, of quantum number I_X

Meaning of symbols (where not otherwise defined in this Table or Section):

τ_c Correlation time for molecular tumbling

τ_e Correlation time related, *inter alia*, to the spin-lattice relaxation time for the unpaired electrons

τ_{sc} For scalar relaxation of the first kind this is the exchange lifetime; for scalar relaxation of the second kind this is T_{1X}

N_X Concentration of spins X (per unit volume)

D Mutual translational self-diffusion coefficient of the molecules containing A and X

a Distance of closest approach of A and X

γ_e Magnetogyric ratio for the electron

a_N Nucleus-electron hyperfine splitting constant (in frequency units)

C Spin-rotation interaction constant (assumed to be isotropic)

$\Delta\sigma$ Shielding anisotropy ($\sigma_{||} - \sigma_{\perp}$; see Section 6-6)

5.3. Relaxation mechanisms.

The combined effect of different relaxation mechanisms is found by summing the relaxation rates (i.e.

$$\frac{1}{T_1} = \left(\frac{1}{T_1}\right)_{hom} + \left(\frac{1}{T_1}\right)_{het-d} + \left(\frac{1}{T_1}\right)_{ue-dd} + \dots$$

A few general inferences can be drawn from this table: (i) relaxation due to dipole-dipole coupling is very sensitive to the inter-nuclear separation (scales as r^{-6}); (ii) the dependence on $\gamma_A^2 \gamma_X^2$ means that the effects of ${}^1\text{H}$ nuclei generally dominate relaxation in organic molecules; (iii) similarly the presence of any unpaired electron has a very strong effect on relaxation (e.g. use of paramagnetic contrast agents, such as gadolinium chelates in MRI)

5.3. Relaxation mechanisms.

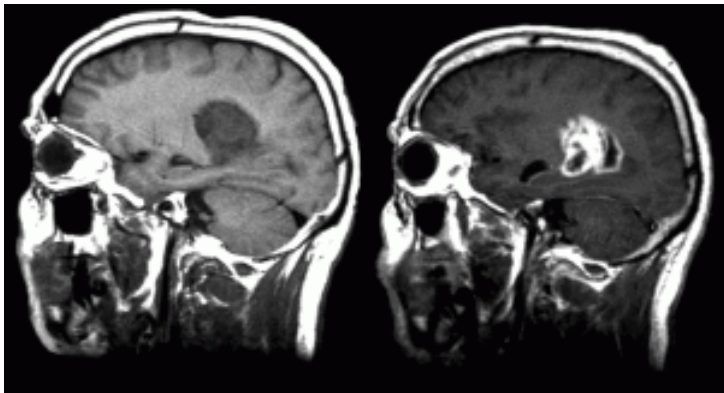


Fig.39: MR images acquired before (left) and after (after) administration of a gadolinium-based contrast agent. The contrast agent reduces T_1 which enhances the contrast. Contrast agent accumulated in a tumour as a result of break-down of the blood-brain barrier (home.physics.wisc.edu).

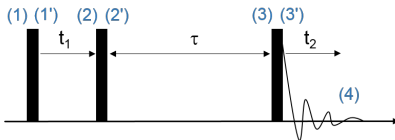
Summary of Lecture 8.

- T_1 and T_2 relaxation arise due to fluctuations of the local magnetic field, caused by molecular motions.
 - the relaxation rates can be calculated using time-dependent perturbation theory
 - there is variety of relaxation mechanisms
- Suggested reading:** Harris 3.14, 3.15, 3.16

2D NMR basics.

- Exchange experiment.
- Relaxation due to dipole-dipole coupling.
- NOESY experiment.

6.1. Exchange experiment.



(1')	$M_y = I_A$ $M_x = 0$	$M_y = I_B$ $M_x = 0$
(2)	$M_y = I_A \cos \omega_A t_1$ $M_x = I_A \sin \omega_A t_1$	$M_y = I_B \cos \omega_B t_1$ $M_x = I_B \sin \omega_B t_1$
(2')	$M_z = I_A \cos \omega_A t_1$ $M_x = I_A \sin \omega_A t_1$	$M_z = I_B \cos \omega_B t_1$ $M_x = I_B \sin \omega_B t_1$
(3)	$M_z = I_A(1 - \delta) \cos \omega_A t_1 + I_B \delta \cos \omega_B t_1$	$M_z = I_B(1 - \delta) \cos \omega_B t_1 + I_A \delta \cos \omega_A t_1$
(3')	$M_y = I_A(1 - \delta) \cos \omega_A t_1 + I_B \delta \cos \omega_B t_1$	$M_y = I_B(1 - \delta) \cos \omega_B t_1 + I_A \delta \cos \omega_A t_1$
(4)	$M_y = (I_A(1 - \delta) \cos \omega_A t_1 + I_B \delta \cos \omega_B t_1) \times \cos \omega_A t_2$ $M_x = (I_A(1 - \delta) \cos \omega_A t_1 + I_B \delta \cos \omega_B t_1) \times \sin \omega_A t_2$	$M_y = (I_B(1 - \delta) \cos \omega_B t_1 + I_A \delta \cos \omega_A t_1) \times \cos \omega_B t_2$ $M_x = (I_B(1 - \delta) \cos \omega_B t_1 + I_A \delta \cos \omega_A t_1) \times \sin \omega_B t_2$

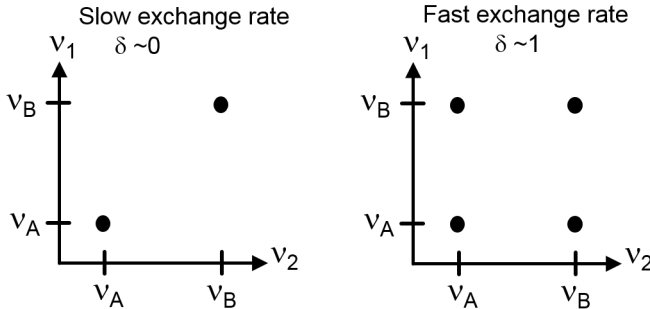
The detected signal is:

$$\begin{aligned} S(t_1, t_2) &\sim M_y(t_1, t_2) = \\ &= (I_A(1 - \delta) \cos \omega_A t_1 + I_B \delta \cos \omega_B t_1) \times \cos \omega_A t_2 \\ &+ (I_B(1 - \delta) \cos \omega_B t_1 + I_A \delta \cos \omega_A t_1) \times \cos \omega_B t_2 \end{aligned}$$

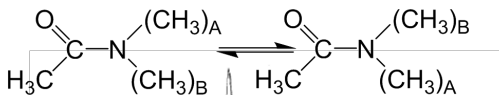
6.1. Exchange experiment.

$$\begin{aligned} S(t_1, t_2) &\sim M_y(t_1, t_2) = \\ &= (I_A(1 - \delta) \cos \omega_A t_1 + I_B \delta \cos \omega_B t_1) \times \cos \omega_A t_2 \\ &+ (I_B(1 - \delta) \cos \omega_B t_1 + I_A \delta \cos \omega_A t_1) \times \cos \omega_B t_2 \end{aligned}$$

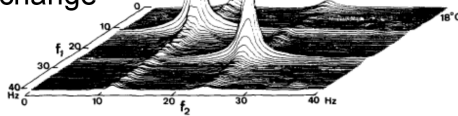
After a Fourier transform in both t_1, t_2 dimensions (since we detect only M_y , this would be a cosine FT) we peaks in a 2D (ν_1, ν_2) -plane.



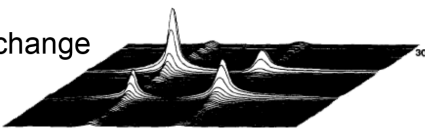
6.1. Exchange experiment.



Slow exchange rate



Faster exchange rate



The experimental scheme described above is very general and is applied in a variety of other experiments. One particular experiment is **NOESY**, Nuclear Overhauser Effect Spectroscopy,

6.2. Relaxation due to dipole-dipole coupling.

In this section we will consider the relaxation (cross-relaxation) due to time-varying dipole-dipole interaction in a heteronuclear AX dipolar coupled spin- $\frac{1}{2}$ system.

Transitions	Dipolar Terms	Transition Rate	Spectral Density
$ \alpha\alpha\rangle \leftrightarrow \beta\alpha\rangle$	C, D	$W_{1A} (= W_{13}, W_{23})$	$J(\omega_A)$
$ \alpha\beta\rangle \leftrightarrow \beta\beta\rangle$	C, D	$W_{1X} (= W_{12}, W_{34})$	$J(\omega_X)$
$ \alpha\beta\rangle \leftrightarrow \beta\alpha\rangle$	B	$W_0 (= W_{23})$	$J(\omega_A - \omega_X)$
$ \alpha\alpha\rangle \leftrightarrow \beta\beta\rangle$	E, F	$W_2 (= W_{14})$	$J(\omega_A + \omega_X)$

Fig.1: Transitions, relevant dipolar terms, transition rates and relevant spectral density for heteronuclear dipole-dipole coupling of an AX system

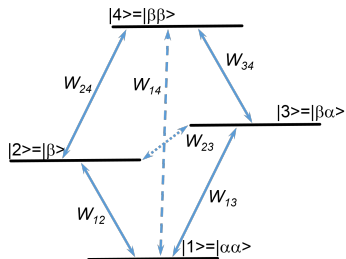


Fig.40: Energy levels and transition in dd-coupled AX system.

6.2. Relaxation due to dipole-dipole coupling.

To find the transition rate we used time-dependent perturbation theory as before, which for example, gives for W_0 :

$$\begin{aligned} W_0 &= \int_{-\infty}^{\infty} \overline{\langle \beta\alpha | \hat{H}_{dd}(t+\tau) | \alpha\beta \rangle \langle \beta\alpha | \hat{H}_{dd}(t) | \alpha\beta \rangle} e^{-i(\omega_A - \omega_X)\tau} d\tau = \\ &= \frac{1}{16} \left(\frac{\mu_0 \gamma_A \gamma_X \hbar}{4\pi r^3} \right)^2 | \langle \beta\alpha | \hat{l}_{1+} \hat{l}_{2-} + \hat{l}_{1-} \hat{l}_{2+} | \alpha\beta \rangle |^2 \langle (3\cos^2\theta - 1)^2 \rangle J(\omega_A - \omega_X) \end{aligned} \quad (12)$$

Using $\langle (3\cos^2\theta - 1)^2 \rangle = \frac{4}{5}$, $\langle \sin^2\theta \cos^2\theta \rangle = \frac{2}{15}$, and $\langle \sin^4\theta \rangle = \frac{8}{15}$ we obtain:

$$\begin{aligned} W_0 &= \frac{1}{20} \left(\frac{\mu_0 \gamma_A \gamma_X \hbar}{4\pi r^3} \right)^2 J(\omega_A - \omega_X) \\ W_{1A} &= \frac{3}{40} \left(\frac{\mu_0 \gamma_A \gamma_X \hbar}{4\pi r^3} \right)^2 J(\omega_A) \\ W_{1X} &= \frac{3}{40} \left(\frac{\mu_0 \gamma_A \gamma_X \hbar}{4\pi r^3} \right)^2 J(\omega_X) \\ W_2 &= \frac{3}{10} \left(\frac{\mu_0 \gamma_A \gamma_X \hbar}{4\pi r^3} \right)^2 J(\omega_A + \omega_X) \end{aligned} \quad (124)$$

6.2. Relaxation due to dipole-dipole coupling.

To establish the relationship between transition rates and T_1 -relaxation, we consider the "rate equations" describing populations of the different states. For example, for the population of the $|\alpha\alpha\rangle$ state, $n_{\alpha\alpha}$, which has an equilibrium value of $n_{\alpha\alpha}^0$, we see that:

$$\begin{aligned}\frac{dn_{\alpha\alpha}}{dt} = & -(W_{1A} + W_{1X} + W_2)(n_{\alpha\alpha} - n_{\alpha\alpha}^0) + W_2(n_{\beta\beta} - n_{\beta\beta}^0) + \\ & + W_{1A}(n_{\beta\alpha} - n_{\alpha\beta}^0) + W_{1X}(n_{\beta\alpha} - n_{\alpha\beta}^0)\end{aligned}\quad (125)$$

Similar expressions can be derived for the rate of exchange of $n_{\beta\beta}$, $n_{\beta\alpha}$ and $n_{\alpha\alpha}$, and writing:

$$\begin{aligned}N_A &= (n_{\alpha\alpha} - n_{\beta\alpha}) + (n_{\alpha\beta} - n_{\beta\beta}) \\ N_X &= (n_{\alpha\alpha} - n_{\alpha\beta}) + (n_{\beta\alpha} - n_{\beta\beta})\end{aligned}\quad (126)$$

to represent the population differences of the A and X spins, respectively, we find:

$$\begin{aligned}\frac{dN_A}{dt} &= -(W_0 + 2W_{1A} + W_2)(N_A - N_A^0) - (W_2 - W_0)(N_X - N_X^0) \\ \frac{dN_X}{dt} &= -(W_0 + 2W_{1X} + W_2)(N_X - N_X^0) - (W_2 - W_0)(N_A - N_A^0)\end{aligned}\quad (127)$$

6.2. Relaxation due to dipole-dipole coupling.

These are known as **Solomon equations**. The first term in each of these equations reflects **auto-relaxation**, while the second terms relates to **cross-relaxation** which links X -spin and A -spin population differences. This yields a value for the auto T_1 -relaxation rate of the A spin population due to heteronuclear dipole-dipole coupling as:

$$\begin{aligned}\frac{1}{T_{1A}} &= W_0 + 2W_{1A} + W_2 = \\ &= \frac{1}{20} \left(\frac{\mu_0 \gamma_A \gamma_X \hbar}{4\pi r^3} \right)^2 (J(\omega_A - \omega_X) + 3J(\omega_A) + 6J(\omega_A + \omega_X))\end{aligned}\tag{128}$$

which in the extreme narrowing limit ($| \omega_A \pm \omega_X |, \omega_A, \omega_X \ll \tau_c^{-1}$) becomes

$$\frac{1}{T_{1A}} = \left(\frac{\mu_0 \gamma_A \gamma_X \hbar}{4\pi r^3} \right)^2 \tau_c\tag{129}$$

6.2. Relaxation due to dipole-dipole coupling.

A similar analysis focusing on the evolution of $N_A + N_X$ gives the value of T_1 due to homonuclear dipole-dipole coupling as:

$$\frac{1}{T_1} = 2(W_1 + W_2) = \frac{3}{20} \left(\frac{\mu_0 \gamma_A \gamma_X \hbar}{4\pi r^3} \right)^2 (J(\omega_0) + 4J(2\omega_0)) \quad (130)$$

In the extreme narrowing limit the latter takes form:

$$\frac{1}{T_1} = \frac{3}{2} \left(\frac{\mu_0 \gamma_A \gamma_X \hbar}{4\pi r^3} \right)^2 \tau_c \quad (131)$$

6.2. Relaxation due to dipole-dipole coupling.

The differences between the homonuclear and heteronuclear expressions arise because of the different effects of the flip-flop (B) term in the dipole-dipole Hamiltonian.

The cross-relaxation rate for the heteronuclear dipole-dipole coupling is:

$$(W_0 - W_2) = \frac{1}{20} \left(\frac{\mu_0 \gamma_A \gamma_X \hbar}{4\pi r^3} \right)^2 (J(\omega_A - \omega_X) - 6J(\omega_A + \omega_X)) \quad (132)$$

6.2. Relaxation due to dipole-dipole coupling.

The rate of change of the average magnetization of one spin as a result of cross-relaxation from a spin to which it is coupled by dipolar effects depends on the cross-relaxation rate, which for homonuclear coupling takes a values of

$$W_0 - W_2 = \frac{1}{20} \left(\frac{\mu_0 \gamma_A \gamma_X \hbar}{4\pi r^3} \right)^2 (J(0) - 6J(2\omega_0)) \quad (133)$$

the dependence on r^6 means that this rate is very strongly dependent on the spatial separation of the coupled nuclei and such cross-relaxation effects will be dominated by nearby nuclei.

6.3. NOESY experiment.

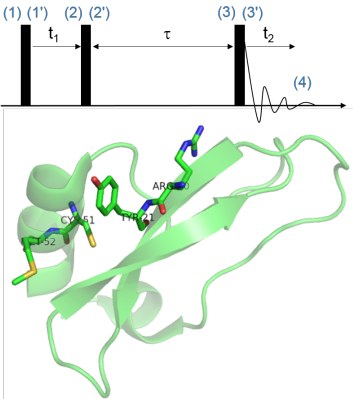
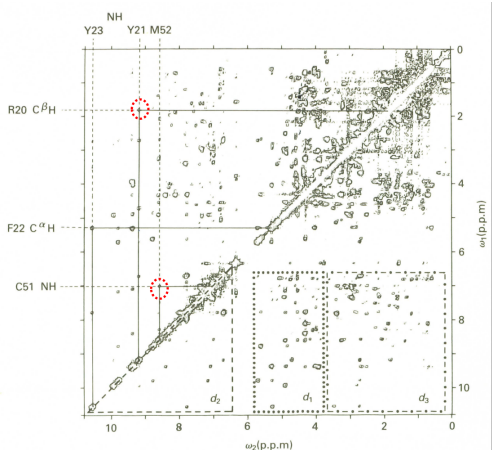


Fig.41: 2D NOESY spectrum of BPTI protein.

6.3. NOESY experiment.

This effect is exploited in the **NOESY (Nuclear Overhauser Effect)** 2D-NMR spectroscopy technique, in which cross-peaks between nearby ^1H sites in large molecules in solution are generated as a result of cross-relaxation and the amplitude of these peaks give an indication of the rate of cross-relaxation and thus the distance between the coupled ^1H nuclei.

NOESY exploits magnetization exchange pulse sequence discussed earlier.

NOESY is a key technique for the determination of protein structure, since it provides constraints on distances between ^1H atoms in different regions of the molecules.

Summary of Lecture 9.

- Exchange experiment pulse sequence is one of the simplest 2D NMR experiments, and forms the basis for many pulse NMR experiments.
- Dipole-dipole cross-relaxation is very pronounced process in liquids and present a form of magnetization "exchange" between nuclei
- NOESY experiment is a key experiment in protein NMR allowing to probe the contacts in protein.

Suggested reading: Harris SSS

Magnetic Resonance Imaging.

- Magnetic Field Gradient.
- Simple 2D MRI.
- Slice Selection.

7.1. Magnetic Field Gradient.

Magnetic field gradients are used for spatial encoding of the NMR signal in MRI.

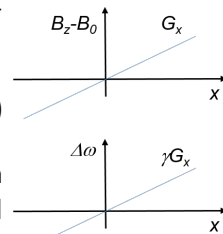
Magnetic field gradient is an additional magnetic field whose z-component (parallel to the strong static field, B_0) varies linearly with spatial position -e.g. for an x -gradient.

$$B_z = B_0 + G_x x, \quad (134)$$

where G_x is the gradient strength in Tesla per meter (Tm^{-1}). This means that the Larmor frequency varies with position as:

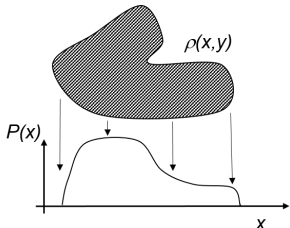
$$\omega = \gamma B_z = \omega_0 + \Delta\omega \quad (135)$$

with $\Delta\omega = \gamma G_x x$. In the presence of an x -gradient, the frequency of the NMR signal therefore indicates the x -position of the signal sources. This is the basis of MRI.



7.2. Simple 2D MRI.

Let's consider a simple two dimensional 2D object, $\rho(x, y)$ from which we want to make a 2D image. Here $\rho(x, y)$ is known as the "spin density" and indicates the number of hydrogen nuclei at location (x, y) .



If we apply a 90° RF pulse and then acquire the NMR signal from the object in the presence of an x -gradient, the signal (neglecting relaxation) is :

$$S(t) = \int_{-\infty}^{\infty} dx \int_{-\infty}^{\infty} dy \rho(x, y) e^{i\gamma G_x x t} = \int_{-\infty}^{\infty} dx P(x) e^{i\gamma G_x x t}, \quad (136)$$

where $P(x) = \int_{-\infty}^{\infty} \rho(x, y) dy$ is the x -profile of the object.

7.2. Simple 2D MRI.

Consequently, the Fourier transform of the signal acquired under an x -gradient, yields the 1D x -profile of the object, because:

$$\begin{aligned} F(\omega) &= \int_{-\infty}^{\infty} dt S(t) e^{-i\omega t} = \\ &= \int_{-\infty}^{\infty} dt \int_{-\infty}^{\infty} dx P(x) e^{i\gamma G_x x t} e^{-i\omega t} = P\left(\frac{\omega}{\gamma G_x}\right) \quad (137) \end{aligned}$$

The first MRI images were generated by measuring profiles of the object along different directions. This involves acquiring the NMR signal multiple time with the gradient applied at different angles with respect to the object. The profiles can be recombined by "filter back projection" as used in original CT and PET systems. Such approach is still used in EPR-based imaging.

7.2. Simple 2D MRI.

In the original experiment Lauterbur used two thin-walled 1 mm diameter glass capillaries of H₂O inside a 4.2 mm glass tube with D₂O.

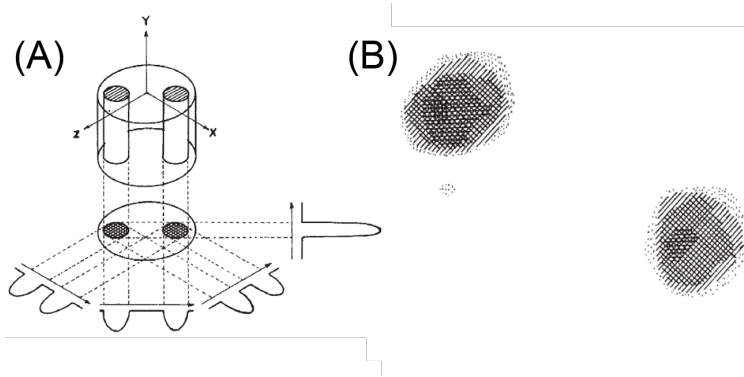


Fig.42: (A) Relationship between a three-dimensional object, its two-dimensional projection along the Y-axis and four one-dimensional projections at 45° intervals in the XZ-plane. (B) Proton density image based on four projections shown in (A). Source: Lauterbur, *Nature* 242, 190

7.2. Simple 2D MRI.

Images are now more commonly generated by using 2D-Fourier Transform (2DFT) sequences. In this approach, a gradient is applied in the y -direction ($\Delta B = G_y y$) for a time, t_y , after the RF pulse, before the NMR signal is acquired under the x - gradient, over time, t_x . In this case the signal is given by

$$S(t_x, t_y) = \int_{-\infty}^{\infty} dx \int_{-\infty}^{\infty} dy \rho(x, y) e^{i\gamma G_x x t_x} e^{i\gamma G_y y t_y} \quad (138)$$

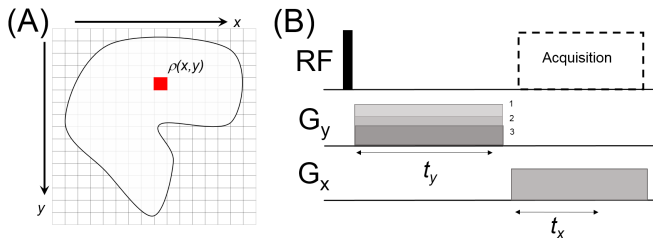


Fig.43: (A) Various locations of an object acquire phases determined by their coordinates, (B) a simple 2DFT sequence

7.2. Simple 2D MRI.

By considering the signal contribution from location $(x, y) = \rho(x, y)e^{i\gamma G_x xt_x}e^{i\gamma G_y yt_y}$, we see that the *frequency* of the signal $\gamma G_x xt_x$ depends on the x -position of the source, while the *phase* of the signal $\gamma G_y yt_y$ depends on the y -position of the source. If the sequence is repeated multiple times using different values of G_y , we can stack up the signals and then Fourier transform with respect to $\gamma G_y t_y$ and $\gamma G_x t_x$ to yield a 2D image.

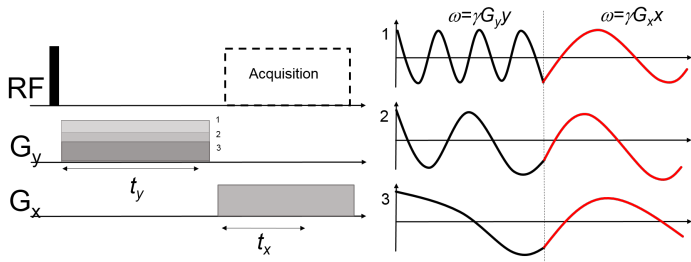


Fig.44: (A) a simple 2DFT sequence (B) Schematic signals at various y -gradient strength

7.2. Simple 2D MRI.

Some additional notes:

In this example the x -gradient is said to produce **frequency encoding** and y -gradient produces **phase encoding** of the signal.

For convenience we can rewrite Eq.138 by replacing $k_x = G_x t_x$ and $k_y = G_y t_y$:

$$S(k_x, k_y) = \int_{-\infty}^{\infty} dx \int_{-\infty}^{\infty} dy \rho(x, y) e^{ik_x x} e^{ik_y y} \quad (139)$$

The density can therefore be obtained via an inverse Fourier Transform:

$$\rho(x, y) = \int_{-\infty}^{\infty} dk_x \int_{-\infty}^{\infty} dk_y S(k_x, k_y) e^{-ik_x x} e^{-ik_y y} \quad (140)$$

7.3. Slice Selection.

To make a useful 2D MR image of a 3D object, it is necessary to map the signal only from a thin section of the object.

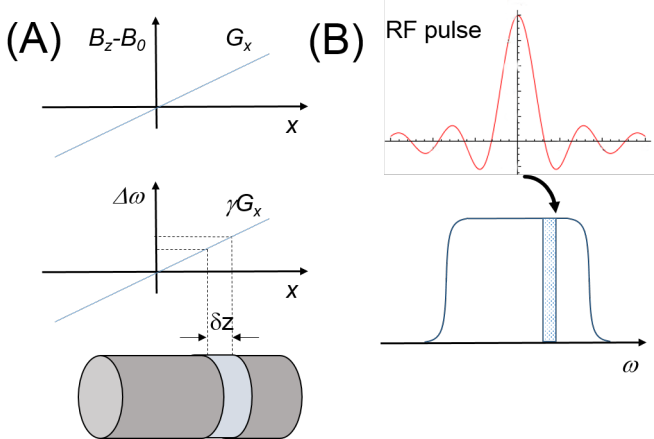


Fig.45: (A) signals of an object in a magnetic field gradient (B) Excitation of a slice using a shaped pulse.

7.3. Slice Selection.

This is accomplished by selectively "exciting" the signal from a slice, by applying a "shaped" RF pulse in conjunction with a magnetic field gradient along the direction perpendicular to the slice. Nuclear magnetization is unaffected by RF that is applied significantly off resonance. Therefore, applying a 90° RF pulse that only contains a range of angular frequencies ($\delta\omega$), around ω_0 , only rotates the magnetization whose resonance frequency is in this range from longitudinal to transverse. In the presence of a gradient along z , $\Delta\omega = \gamma G_z z$, so the magnetization in a range of z values, $\delta z = \frac{\delta\omega}{\gamma G_z}$, is excited and generates a signal. This is known as slice selection.

7.3. Slice Selection.

Bringing together slice selection, phase encoding and frequency encoding, produces a powerful and versatile approach to MRI.

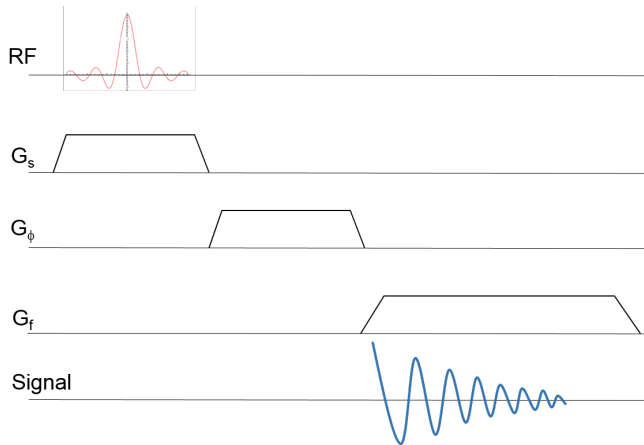


Fig.46: A typical pulse imaging pulse sequence employing a RF pulse with G_s gradient, a phase encoding gradient G_ϕ , and frequency-encoding gradient G_f .

7.3. Slice Selection.

The appearance of MR images ("contrast") can be easily changed by exploiting sensitivity to the NMR relaxation times, T_1 , T_2 (e.g. by using a spin echo or inversion recovery sequence in conjunction with imaging)

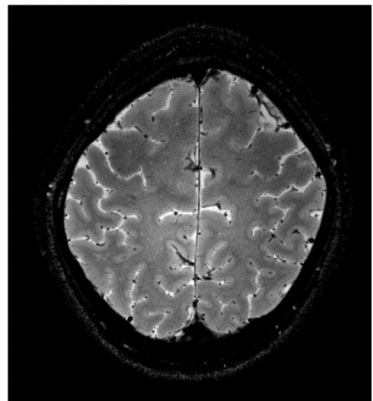
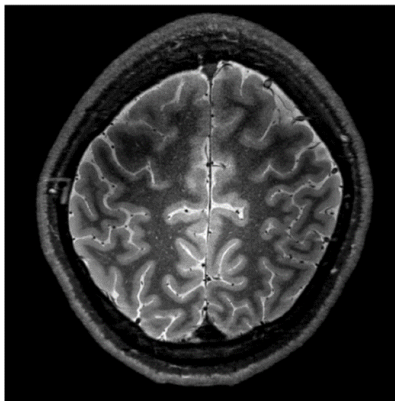


Fig.47: Example high resolution brain images obtained at 7T with (A) T_1 -weighting and (B) T_2 -weighting.

Summary of lecture 10.

- Magnetic field gradients are essential for MRI, they relate the Larmor frequency with a physical location of an object.
- Projection reconstruction was used in early MRI, now gradient-based pulse sequences allow recording a multidimensional signal used for reconstructing the density.
- A typical 3D imaging experiment employs slice-selection, phase and frequency encoding.

Suggested reading: for more on this read Ch.9 and 10, Magnetic Resonance Imaging: Physical Principles and Sequence design, by Brown et al. (online text is available at UoN library).